

# BART-based inference for Poisson processes

Stamatina Lamprinakou<sup>1,\*</sup>, Emma McCoy<sup>1</sup>, Mauricio Barahona<sup>1</sup>, Axel Gandy<sup>1</sup>,  
Seth Flaxman<sup>1</sup>, and Sarah Filippi<sup>1</sup>

<sup>1</sup>Department of Mathematics, Imperial College London, London, United Kingdom

\*Corresponding author: s.lamprinakou18@imperial.ac.uk

May 19, 2020

## Abstract

The effectiveness of Bayesian Additive Regression Trees (BART) has been demonstrated in a variety of contexts including non parametric regression and classification. Here we introduce a BART scheme for estimating the intensity of inhomogeneous Poisson Processes. Poisson intensity estimation is a vital task in various applications including medical imaging, astrophysics and network traffic analysis. Our approach enables full posterior inference of the intensity in a nonparametric regression setting. We demonstrate the performance of our scheme through simulation studies on synthetic and real datasets in one and two dimensions, and compare our approach to alternative approaches.

## 1 Introduction

The Bayesian Additive Regression Trees (BART) model is a Bayesian framework related to random forests, which uses a sum of trees to predict the mean of a response  $Y$  given covariates  $X$ . The Bayesian approach imposes a prior on all parameters of the model, including the trees. A regularization prior is imposed on trees such that each tree behaves as a weak learner, thus achieving a good bias-variance trade-off. Chipman *et al.* (2010) proposed an inference procedure using Metropolis Hastings within a Gibbs Sampler, whereas Lakshminarayanan *et al.* (2015) used a Particle Gibbs Sampler to increase mixing when the true posterior consists of deep trees or when the dimensionality of the data is high. Several theoretical studies of BART models (Rockova and van der Pas, 2017; Rockova and Saha, 2018; Linero and Yang, 2018) have recently established optimal posterior convergence rates. The BART model has been applied in various contexts including nonparametric mean regression (Chipman *et al.*, 2010), classification (Chipman *et al.*, 2010; Zhang and Härdle, 2010; Kindo *et al.*, 2016), variable selection (Chipman *et al.*, 2010; Bleich *et al.*, 2014; Linero, 2018), estimation of monotone functions (Chipman *et al.*, 2016), causal inference (Hill, 2011), survival analysis (Sparapani *et al.*, 2016), and heteroskedasticity (Bleich and Kapelner, 2014). Linero and Yang (2018) illustrated how the BART model suffers from a lack of smoothness and the curse of dimensionality, and overcome both potential shortcomings by considering a sparsity assumption similar to (Linero, 2018) and treating decisions at branches probabilistically.

The original BART model (Chipman *et al.*, 2010) has a Gaussian assumption and hence the majority of applications of BART have been restricted to Gaussian data. Murray (2017) adapted BART to model count responses via a log-linear transformation, and provided

an efficient MCMC sampler for categorical and count responses. Our focus here is on extending this methodology to estimate the intensity function of Poisson processes in an inhomogeneous setting.

The question of estimating the intensity of Poisson processes has a long history, including both frequentist and Bayesian methods. Frequentist methods include fixed-bandwidth and adaptive bandwidth kernel estimators with edge correction (Diggle *et al.*, 2003), and wavelet-based methods (e.g. Fryzlewicz and Nason (2004), Patil *et al.* (2004)). Bayesian methods include using a sigmoidal Gaussian Cox process model for intensity inference (Adams *et al.*, 2009), variational Bayesian intensity inference (Lloyd *et al.*, 2015), and non-parametric Bayesian estimations of the intensity via piecewise functions with either random or fixed partitions of constant intensity (Arjas and Gasbarra, 1994; Heikkinen and Arjas, 1998; Gugushvili *et al.*, 2018).

In this paper, we introduce an extension of the BART model (Chipman *et al.*, 2010) for Poisson Processes whose intensity at each point is estimated via an ensemble of trees. Specifically, the logarithm of the intensity at each point is modelled via a sum of trees (and hence the intensity is a product of trees). This approach enables full posterior inference of the intensity in a nonparametric regression setting. Our main contribution is a novel BART scheme for estimating the intensity of inhomogeneous Poisson Processes. The simulation studies demonstrate that our algorithm is competitive with the Haar-Fisz algorithm and kernel approaches. We also demonstrate its ability to track a varying intensity in synthetic and real data.

The outline of the article is as follows. Section 2 introduces our approach for estimating the intensity of a Poisson process through the BART model, and Section 3 presents the proposed inference algorithm. Sections 4 and 5 present the application of the algorithm to synthetic data and real data sets, respectively. Section 6 provides our conclusions and plans for future work.

## 2 The BART Model for Poisson Processes

Consider an inhomogeneous Poisson process defined on a  $d$ -dimensional domain  $S \subset \mathbb{R}^d$ ,  $d \geq 1$ , with intensity  $\lambda : S \rightarrow \mathbb{R}^+$ . For such a process, the number of points within a subregion  $B \subset S$  has a Poisson distribution with intensity  $\lambda_B = \int_B \lambda(s) ds$ , and the number of points in disjoint subregions are independent (Daley and Vere-Jones, 2003). Clearly, the homogeneous Poisson process is the special case with constant intensity function  $\lambda(s) = c$ ,  $\forall s \in S$ .

To estimate the intensity of the inhomogeneous Poisson process, we use  $m$  partitions of the domain  $S$ , each associated with a tree  $T_h$ ,  $h = 1, \dots, m$ . The partitions are denoted  $T_h = \{\Omega_{ht}\}_{t=1}^{b_h}$ , where  $b_h$  is the number of terminal nodes in the corresponding tree  $T_h$ , and each leaf node  $t$  corresponds to one of the subregions  $\Omega_{ht}$  of the partition  $T_h$ . Each subregion  $\Omega_{ht}$  has an associated parameter  $\lambda_{ht}$ , and hence each tree  $T_h$  has an associated vector of leaf intensities  $\Lambda_h = (\lambda_{h1}, \lambda_{h2}, \dots, \lambda_{hb_h})$ .

We model the intensity of  $s \in S$  as:

$$\log(\lambda(s)) = \sum_{h=1}^m \sum_{t=1}^{b_h} \log(\lambda_{ht}) I(s \in \Omega_{ht}) \quad (1)$$

$$T_h \sim \text{heterogeneous Galton-Watson process for a partition of } S \quad (2)$$

$$\lambda_{ht} | T_h \sim \text{Gamma}(\alpha, \beta) \quad (3)$$

where  $I(\cdot)$  denotes the indicator function. It follows immediately from (1) that the intensity of the process can be expressed as a product of trees:

$$\lambda(s) = \prod_{h=1}^m \prod_{t=1}^{b_h} \lambda_{ht}^{I(s \in \Omega_{ht})}. \quad (4)$$

Given a fixed number of trees,  $m$ , the parameters of the model are thus the regression trees  $T = \{T_h\}_{h=1}^m$  and their corresponding intensities  $\Lambda = \{\Lambda_h\}_{h=1}^m$ . Following Chipman *et al.* (2010), we assume that the tree components  $(T_h, \Lambda_h)$  are independent of each other, and that the terminal node parameters of every tree are independent, so that the prior can be factorized as:

$$P(\Lambda, T) = \prod_{h=1}^m P(\Lambda_h, T_h) = \prod_{h=1}^m P(\Lambda_h | T_h) P(T_h) = \prod_{h=1}^m \left[ \prod_{t=1}^{b_h} P(\lambda_{ht} | T_h) \right] P(T_h). \quad (5)$$

**Prior on the trees.** The trees  $T_h$  of the BART model are stochastic regression trees generated through a heterogeneous Galton-Watson (GW) process (Rockova and Saha, 2018). In our case, we use a GW process in which each node has either zero or two offsprings and the probability of a node splitting depends on its depth in the tree. Specifically, a node  $\eta \in T_h$  splits into two offsprings with probability

$$p_{\text{split}}(\eta) = \frac{\gamma}{(1 + d(\eta))^\delta}, \quad (6)$$

where  $d(\eta)$  is the depth of node  $\eta$  in the tree, and  $\gamma \in (0, 1)$  and  $\delta \geq 0$  are parameters of the model. Classic results from the theory of branching processes show that  $\gamma \leq 0.5$  guarantees that the expected depth of the tree is finite. In our construction, each tree  $T_h$  is associated with a partition of  $S$ . Namely, if node  $\eta$  splits, we select uniformly at random one of the  $d$  dimensions of the space of the Poisson process, followed by uniform selection from the available split values associated with that dimension, consistent with the descendants of node  $\eta$  in the tree.

**Prior on the leaf intensities.** Our choice of a Gamma prior for the leaf parameters  $\lambda_{ht}$  builds upon previous work by Murray (2017), who used a mixture of Generalized Inverse Gaussian (GIG) distributions as the prior on leaf parameters in a BART model for count regression. Here we impose a Gamma prior (a special case of GIG) on the leaf parameters, which simplifies the model and leads to a closed form of the conditional integrated likelihood below (see Section 3).

### 3 The Inference Algorithm

Given a finite realization of an inhomogeneous Poisson process with  $n$  sample points  $s_1, \dots, s_n \in S \subset \mathbb{R}^d$ , we seek to infer the parameters of the model  $(\Lambda, T)$  by sampling from the posterior  $P(\Lambda, T | s_1, \dots, s_n)$ .

Before presenting the sampling algorithm we summarize a preliminary result. To simplify our notation, let us define

$$g(s_i; T_h, \Lambda_h) = \prod_{t=1}^{b_h} \lambda_{ht}^{I(s_i \in \Omega_{ht})},$$

so that Eq. (4) becomes  $\lambda(s_i) = \prod_{h=1}^m g(s_i; T_h, \Lambda_h)$ .

Let us choose any arbitrary tree  $T_h$  in our ensemble  $T$ , and let us denote the set with the rest of the trees as  $T_{(h)} = \{T_j\}_{j=1, j \neq h}^m$  and their leaf parameters as  $\Lambda_{(h)} = \{\Lambda_j\}_{j=1, j \neq h}^m$ . The intersection of all the partitions associated with the trees in  $T_{(h)}$  gives us a global partition  $\{\bar{\Omega}_k^{(h)}\}_{k=1}^{K(T_{(h)})}$  with  $K(T_{(h)})$  subregions (Rockova and van der Pas, 2017).

Then we have the following result.

**Remark 1.** (i) The conditional likelihood of the realization is given by

$$P(s_1, \dots, s_n | \Lambda, T) = c_h \prod_{t=1}^{b_h} \lambda_{ht}^{n_{ht}} e^{-\lambda_{ht} c_{ht}}, \quad (7)$$

with  $c_h = \prod_{i=1}^n \prod_{j=1, j \neq h}^m g(s_i; T_j, \Lambda_j)$ ,

$$c_{ht} = \sum_{k=1}^{K(T_{(h)})} \bar{\lambda}_k^{(h)} |\bar{\Omega}_k^{(h)} \cap \Omega_{ht}|,$$

where  $\bar{\lambda}_k^{(h)} = \prod_{t=1, t \neq h}^m \prod_{l=1}^{b_t} \lambda_{tl}^{I(\Omega_{tl} \cap \bar{\Omega}_k^{(h)} \neq 0)}$ ,  $n_{ht}$  is the cardinality of the set  $\{i : s_i \in \Omega_{ht}\}$ , and  $|\bar{\Omega}_k^{(h)} \cap \Omega_{ht}|$  is the volume of the region  $\bar{\Omega}_k^{(h)} \cap \Omega_{ht}$ .

(ii) For a tree  $h$ , the conditional integrated likelihood obtained by integrating out  $\Lambda_h$  is

$$P(s_1, \dots, s_n | T_h, T_{(h)}, \Lambda_{(h)}) = c_h \left( \frac{\beta^\alpha}{\Gamma(\alpha)} \right)^{b_h} \prod_{t=1}^{b_h} \frac{\Gamma(n_{ht} + \alpha)}{(c_{ht} + \beta)^{n_{ht} + \alpha}}. \quad (8)$$

*Proof.* See Appendices B and C.  $\square$

We now summarize our sampling algorithm. To sample from  $P(\Lambda, T | s_1, \dots, s_n)$ , we implement a Metropolis-Hastings within block Gibbs sampler (Algorithm 1), which requires  $m$  successive draws from  $(T_h, \Lambda_h) | T_{(h)}, \Lambda_{(h)}, s_1, \dots, s_n$ . Note that

$$\begin{aligned} P(T_h, \Lambda_h | T_{(h)}, \Lambda_{(h)}, s_1, \dots, s_n) &= P(T_h | T_{(h)}, \Lambda_{(h)}, s_1, \dots, s_n) P(\Lambda_h | T_h, T_{(h)}, \Lambda_{(h)}, s_1, \dots, s_n) \\ &\propto P(T_h | T_{(h)}, \Lambda_{(h)}, s_1, \dots, s_n) P(s_1, \dots, s_n | \Lambda, T) P(\Lambda_h | T_h) \\ &= P(T_h | T_{(h)}, \Lambda_{(h)}, s_1, \dots, s_n) c_h \prod_{t=1}^{b_h} \lambda_{ht}^{n_{ht}} e^{-\lambda_{ht} c_{ht}} \prod_{t=1}^{b_h} \frac{\beta^\alpha}{\Gamma(\alpha)} \lambda_{ht}^{\alpha-1} e^{-\beta \lambda_{ht}} \\ &\propto P(T_h | T_{(h)}, \Lambda_{(h)}, s_1, \dots, s_n) \prod_{t=1}^{b_h} \lambda_{ht}^{n_{ht} + \alpha - 1} e^{-(c_{ht} + \beta) \lambda_{ht}}, \end{aligned} \quad (9)$$

which follows directly from Bayes' rule and Eqs. (5) and (3).

From (9), it is clear that a draw from  $(T_h, \Lambda_h) | T_{(h)}, \Lambda_{(h)}, s_1, \dots, s_n$  can be achieved in  $(b_h + 1)$  successive steps consisting of:

- sampling  $T_h | T_{(h)}, \Lambda_{(h)}, s_1, \dots, s_n$  using Metropolis-Hastings (Algorithm 2)
- sampling  $\lambda_{ht} | T, \Lambda_{(h)}, s_1, \dots, s_n$  from a Gamma distribution with shape  $n_{ht} + \alpha$  and rate  $c_{ht} + \beta$  for  $t = 1, \dots, b_h$ .

These steps are implemented through Metropolis-Hastings in Algorithm 1. Note also that

$$P(T_h|T_{(h)}, \Lambda_{(h)}, s_1, \dots, s_n) \propto P(s_1, \dots, s_n|T_h, T_{(h)}, \Lambda_{(h)}) P(T_h),$$

so that the conditional integrated likelihood (8) is required to compute the Hastings ratio.

---

**Algorithm 1** Metropolis-Hastings within Gibbs sampler

---

```

for  $t = 1, 2, 3, \dots$  do
  for  $h = 1$  to  $m$  do
    Sample  $T_h^{(t+1)}|s_1, \dots, s_n, \{T_j^{(t+1)}\}_{j=1}^{h-1}, \{T_j^{(t)}\}_{j=h+1}^m, \{\Lambda_j^{(t+1)}\}_{j=1}^{h-1}, \{\Lambda_j^{(t)}\}_{j=h+1}^m$ 
    using Algorithm 2
    for  $k = 1$  to  $b_h$  do
      Sample  $\lambda_{hk}^{(t+1)}|s_1, \dots, s_n, \{T_j^{(t+1)}\}_{j=1}^h, \{T_j^{(t)}\}_{j=h+1}^m, \{\Lambda_j^{(t+1)}\}_{j=1}^{h-1}, \{\Lambda_j^{(t)}\}_{j=h+1}^m$ 
    end for
  end for
end for

```

---

**Algorithm 2** Metropolis-Hastings Algorithm for sampling from the posterior  $P(T_j|s_1, \dots, s_n, T_{(j)}, \Lambda_{(j)})$

---

Generate a candidate value  $T_j^*$  with probability  $q(T_j^*|T_j^{(t)})$ .

Set  $T_j^{(t+1)} = T_j^*$  with probability

$$\alpha(T_j^{(t)}, T_j^*) = \min \left\{ 1, \frac{q(T_j^*|T_j^{(t)})}{q(T_j^{(t)}|T_j^*)} \frac{P(s_1, \dots, s_n|T_j^*, T_{(j)}, \Lambda_{(j)})}{P(s_1, \dots, s_n|T_j^{(t)}, T_{(j)}, \Lambda_{(j)})} \frac{P(T_j^*)}{P(T_j^{(t)})} \right\}$$

Otherwise, set  $T_j^{(t+1)} = T_j^{(t)}$ .

---

The transition kernel  $q$  in Algorithm 2 is chosen from the three proposals: GROW, PRUNE, CHANGE (Chipman *et al.*, 2010; Kapelner and Bleich, 2013). The GROW proposal randomly picks a terminal node, splits the chosen terminal into two new nodes and assigns a decision rule to it. The PRUNE proposal randomly picks a parent of two terminal nodes and turns it into a terminal node by collapsing the nodes below it. The CHANGE proposal randomly picks an internal node and randomly reassigns to it a splitting rule. We describe the implementation of the proposals in Appendix A.

For completeness, in Appendix D we present the full development of the algorithm for inference of the intensity of inhomogeneous Poisson processes via only one tree.

### 3.1 Fixing the hyperparameters of the model

**Hyperparameters of the Gamma distribution for the leaf intensities.** We use a simple data-informed approach to fix the hyperparameters  $\alpha$  and  $\beta$  of the Gamma distribution (3). We discretize the domain into  $N_G$  subregions of equal volume ( $N_G = 100$  works well in practice) and count the number of samples  $s_i$  per subregion. We thus obtain the empirical densities in each of the subregions:  $\xi_i, i = 1, \dots, N_G$ . Given the form of the intensity (4) as a product of  $m$  trees, we consider the  $m$ -th roots  $\Xi = \{\xi_i^{1/m}\}_{i=1}^{N_G}$  as candidates for the intensity of each tree. Taking the sample mean  $\hat{\mu}_\Xi$  and sample variance  $\hat{\sigma}_\Xi^2$ , we choose the model hyperparameters  $\alpha$  and  $\beta$  to correspond to those of a

Gamma distribution with the same mean and variance, i.e.,  $\alpha = \hat{\mu}_{\Xi}^2/\hat{\sigma}_{\Xi}^2$  and  $\beta = \hat{\mu}_{\Xi}/\hat{\sigma}_{\Xi}^2$ , although fixing  $\beta = 1$  can also give good estimates of the intensity. Although setting  $N_G = 100$  leads to convergence in short time and good estimates of the intensity in our simulation studies below, there are other possibilities. Alternatively, we can bin the data based on a criterion that takes into account the number of samples,  $n$ , and the number of dimensions,  $d$ . For example, the number of bins per dimension,  $n_b$ , can be computed as (Scott, 2008; Wand, 1997): (i)  $n_b = \lceil n^{1/(d+1)} \rceil$ , (ii)  $n_b = \lceil n^{1/(d+2)} \rceil$ , or (iii)  $n_b = \max_{k \in \{1, 2, \dots, d\}} \lceil [DR_k \cdot n^{1/(d+2)}] / (2 \cdot \text{IQR}(\{s_{i,k}\})) \rceil$ , where IQR denotes the interquartile range of the sample,  $DR_k$  is the range of the domain in dimension  $k$  (here we scale the initial domain to a unit hypercube so that  $DR_k = 1, \forall k$ ), and by extension  $N_G = n_b^d$ . In our simulation scenarios below, all these approaches lead to comparable convergence times and estimates of the intensity.

**Hyperparameters of the stochastic ensemble of regression trees.** The GW stochastic process that generates our tree ensemble has several hyperparameters. First, we fix the parameters of the node splitting probability (6) to  $\gamma = 0.98$  and  $\delta = 2$ . Second, each of the  $d$  dimensions has to be assigned a grid of split values, from which the subregions of the partition are randomly chosen, yet always respecting the consistency of the ancestors in the tree. Here, we use a simple uniform grid for each of the  $d$ -dimensions (Pratola *et al.*, 2016): we normalize each dimension of the space from  $(0, 1)$  and discretize each dimension into  $N_d$  segments. ( $N_d = 100$  works well in practice and is used throughout our examples.) More sophisticated, data-informed grids are also possible, although using, e.g., the sample points as split values does not improve noticeably the performance in our examples. Finally, the number of trees  $m$  also needs to be fixed. In our examples below, we have checked the performance of our algorithm with varying number of trees  $m = 2 - 50$ . We find that good performance can be achieved with a moderate number of trees,  $m = 4 - 10$  depending on the particular example.

## 4 Simulation Study on Synthetic Data

We first carried out a simulation study on synthetic data to illustrate the performance of Algorithm 1 to estimate the intensity of one dimensional and two dimensional inhomogeneous Poisson processes.

We simulate realizations of Poisson processes on the domain  $[0, 1]^d$  for  $d \in \{1, 2\}$  via thinning (Lewis and Shedler, 1979). The hyperparameters of the model (for the trees and the leaf intensities) are fixed as described in Section 3.1. We initially randomly generate  $m$  trees of zero depth. The probabilities of the proposals in Algorithm 2 are set to:  $P(\text{GROW}) = P(\text{PRUNE}) = 0.4$  and  $P(\text{CHANGE}) = 0.2$ . A testing set  $\{z_i\}$  is defined by uniformly sampling 10000 points in the domain  $[0, 1]^d$ .

We run 3 parallel chains of the same length for at least 100000 iterations in order to increase our confidence in the results. However, our algorithm works well with around 10000 iterations (see section E). We discard their first halves treating the second halves as a sample from the target distribution. We assess chain convergence using the Gelman-Rubin convergence diagnostic (Gelman *et al.*, 1992) applied to the estimated intensity for each point of the testing set, as well as trace plots and autocorrelation plots for some points of the testing set.

At each state  $t$  of a simulated chain we estimate the intensity for each point  $z_i$  by a

product of trees denoted as

$$\widehat{\lambda}^{(t)}(z_i) = \prod_{j=1}^m g(z_i; T_j^{(t)}, \Lambda_j^{(t)}).$$

The induced sequence  $\{\widehat{\lambda}^{(t)}(\cdot)\}_{t=1}^\infty$  for the sequence of draws  $\{(T_1^{(t)}, \Lambda_1^{(t)}), \dots, (T_m^{(t)}, \Lambda_m^{(t)})\}_{t=1}^\infty$  converges to  $P(\widehat{\lambda}(\cdot)|s_1, \dots, s_n)$ . We compute the posterior mean  $E[\widehat{\lambda}(\cdot)|s_1, \dots, s_n]$ , the posterior median of  $\widehat{\lambda}(\cdot)$ , and the highest density interval (hdi) using the function *hdi* provided by the **R** package **bayestestR** (Makowski *et al.*, 2019). To assess the performance of our algorithm, we compute the Average Absolute Error (AAE) of the computed estimate:

$$\text{AAE}(\widehat{\lambda}) = \frac{1}{N_t} \sum_{i=1}^{N_t} |\widehat{\lambda}(x_i) - \lambda(x_i)| \quad (10)$$

and Root Mean Square Error (RMSE):

$$\text{RMSE}(\widehat{\lambda}) = \left( \frac{1}{N_t} \sum_{i=1}^{N_t} (\widehat{\lambda}(x_i) - \lambda(x_i))^2 \right)^{1/2} \quad (11)$$

where  $N_t$  is the number of test points.

For one dimensional processes, we compare the results of Algorithm 1 to the Haar-Fisz algorithm (Fryzlewicz and Nason, 2004), a wavelet based method for estimating the intensity of one dimensional Poisson Processes that outperforms well known competitors. We apply the Haar-Fisz algorithm to the counts of points falling into 256 consecutive intervals using the **R** package **haarfisz** (Fryzlewicz, 2010). Our algorithm is competitive with the Haar algorithm for stepwise and smooth intensity functions.

For two dimensional processes, we compare the results of our algorithm with fixed-bandwidth estimators with edge correction. According to Davies and Baddeley (2018) the choice of the kernel is not of primary importance, so we choose a Gaussian kernel for its wide applicability. The kernel estimators were computed using the **R** package **spatstat** (Baddeley and Turner, 2005). Our algorithm outperforms kernel smoothing for stepwise functions, and is competitive with the kernel approach for a smooth intensity. The convergence criteria included in the Supplementary Material indicate good convergence of the considered chains in the majority of cases.

## 4.1 One dimensional Poisson Process with stepwise intensity

Our first example is a one dimensional Poisson Process with piecewise constant intensity with several steps (Fig. 1). Our algorithm detects the change points and provides good estimates of the intensity and is competitive with the Haar-Fisz algorithm (see Fig. 1) and Tables 1-2). The convergence criteria indicate convergence of the simulated chains for 5 and 7 trees (see Supplementary Material).

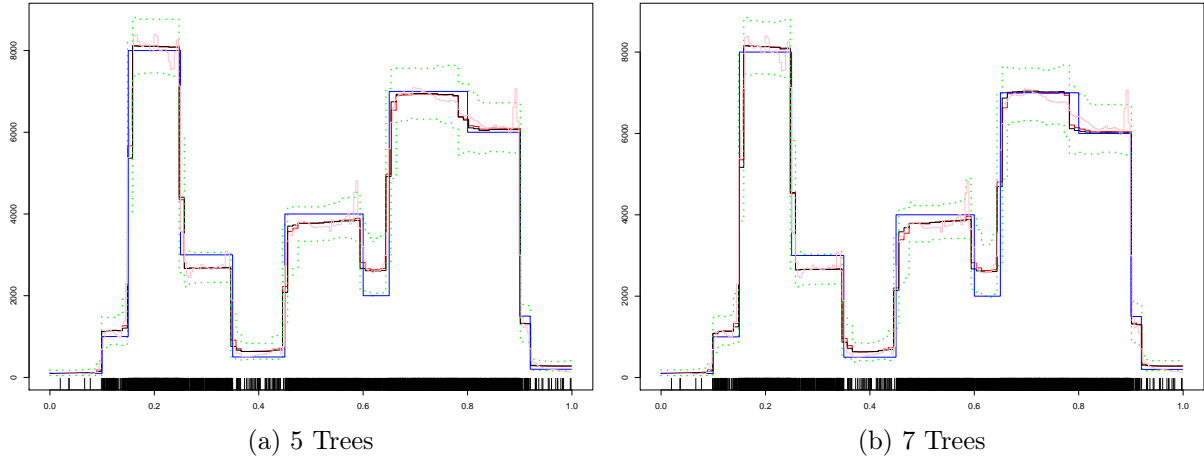


Figure 1: The original intensity (blue curve), the posterior mean (red curve), the posterior median (black curve), the 95% hdi interval of the estimated intensity illustrated by the dotted green lines and the Haar-Fisz estimator (pink curve). The rug plot on the bottom displays the 3590 event times.

Proposed Algorithm				
Number of trees	AAE for Posterior Mean	AAE for Posterior Median	RMSE for Posterior Mean	RMSE for Posterior Median
5	279.88	269.81	572.94	576.94
7	278.37	269.78	582.82	584.1

Table 1: Average Absolute Error and Root Mean Square Error for various number of trees for the data in Fig. 1.

Haar-Fisz Algorithm	
AAE	RMSE
272.26	476.94

Table 2: Average Absolute Error and Root Mean Square Error for Haar-Fisz estimator for the data in Fig. 1.

## 4.2 One dimensional Poisson Process with continuously varying intensity

We have applied our algorithm to samples of a one dimensional Poisson process with intensity  $\lambda(x) = 20e^{-x/5}(5 + 4 \cos(x))$  for  $x \in [0, 10]$ . Figure 2 and Tables 3-4 show that the algorithm works well on a smoothly varying intensity with fewer sample points and outperforms the Haar-Fisz Estimator for the majority the range. The convergence criteria indicate convergence of the simulated chains for 10 Trees and for the most testing points for 5 Trees (see supplementary material).

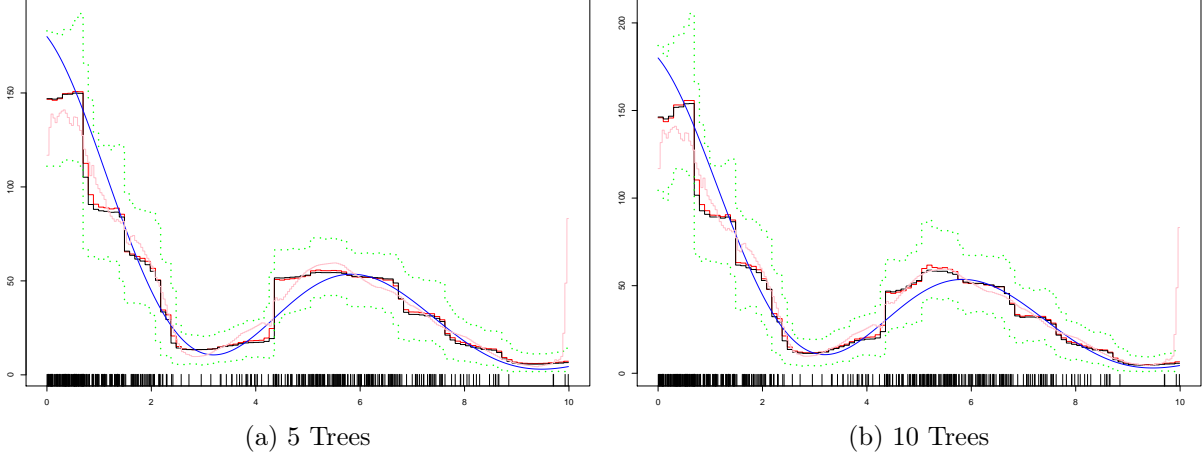


Figure 2: Scenario 2: The original intensity (blue curve), the posterior mean (red curve), the posterior median (black curve), the 95% hdi interval of the estimated intensity illustrated by the dotted green lines and the Haar-Fisz estimator (pink curve). The rug plot on the bottom displays the 440 event times.

Proposed Algorithm				
Number of trees	AAE for Posterior Mean	AAE for Posterior Median	RMSE for Posterior Mean	RMSE for Posterior Median
5	6.14	6.38	9.52	10.17
10	5.95	6.01	9.39	9.8

Table 3: Average Absolute Error and Root Mean Square Error for various number of trees for the data in Fig. 2.

Haar-Fisz Algorithm	
AAE	RMSE
7.16	11.67

Table 4: Average Absolute Error and Root Mean Square Error for Haar-Fisz estimator for the data in Fig. 2

### 4.3 Two dimensional Poisson process with stepwise intensity function

To demonstrate the applicability of our algorithm in a two dimensional setting, Figure 3 and Tables 5-6 reveal that our algorithm outperforms kernel smoothing for stepwise intensity functions. However, as maybe expected, the simulation study shows that points close to jumps are estimated with less reliability. We also note that the chain converges less well at these points as demonstrated by the Gelman-Rubin diagnostic (see supplementary material).

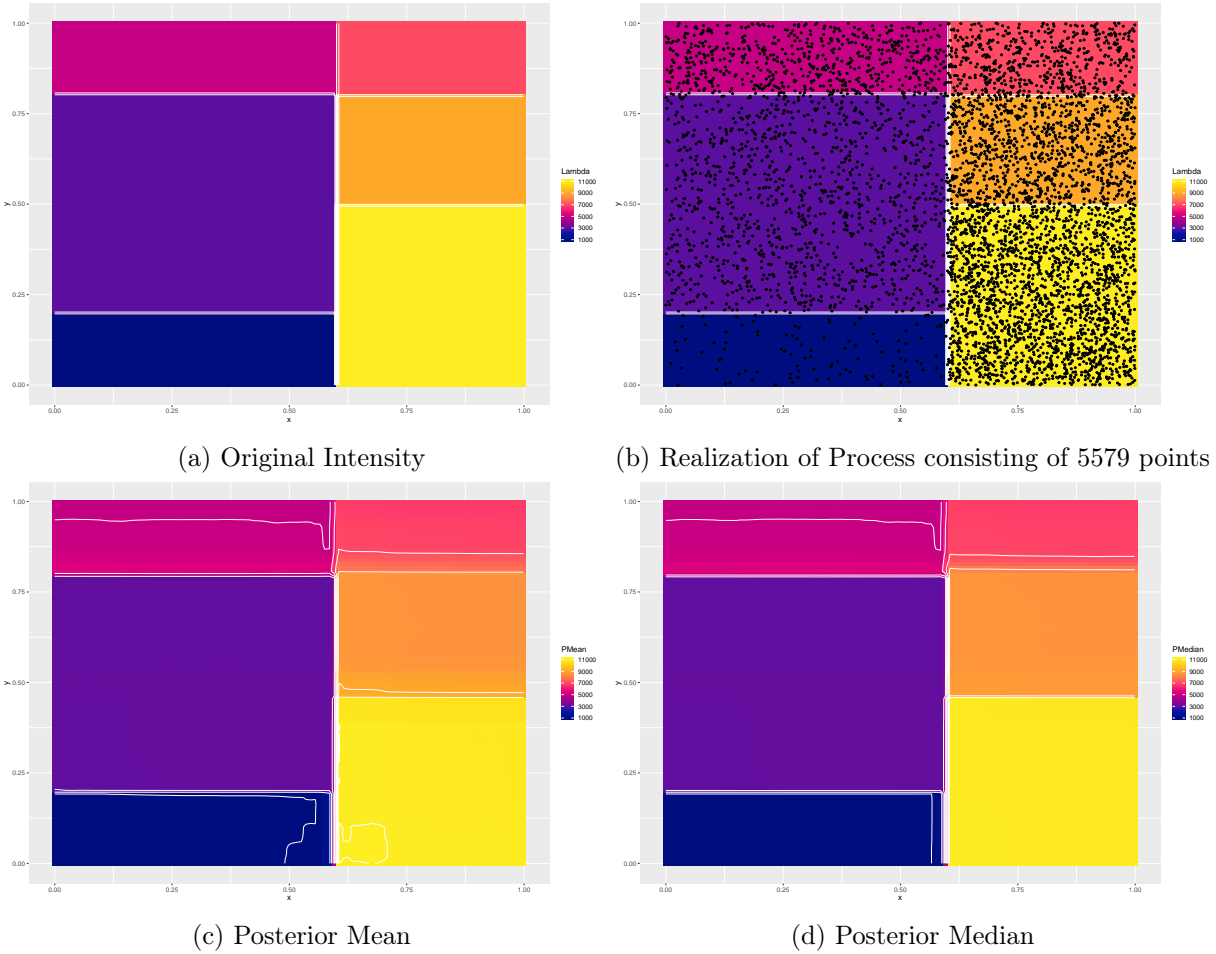


Figure 3: Original Intensity, posterior mean and posterior median for 4 trees.

Proposed Algorithm				
Number of trees	AAE for Posterior Mean	AAE for Posterior Median	RMSE for Posterior Mean	RMSE for Posterior Median
4	208.74	213.04	410.19	447.86

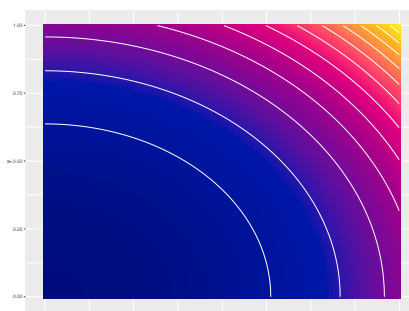
Table 5: Average Absolute Error and Root Mean Square Error for 4 trees for the data in Figure 3.

Kernel Smoothing		
Bandwidth (sigma)	AAE	RMSE
0.027	763.8	1041.26
0.038	662.67	956.84
0.047	636.72	960.59
0.067	672.76	1042.53

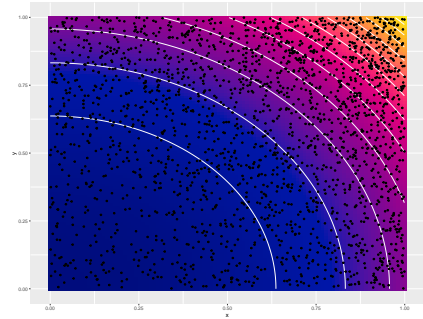
Table 6: Average Absolute Error and Root Mean Square Error for fixed bandwidth estimators for the data in Figure 3.

#### 4.4 Inhomogeneous two dimensional Poisson Process with Gaussian intensity

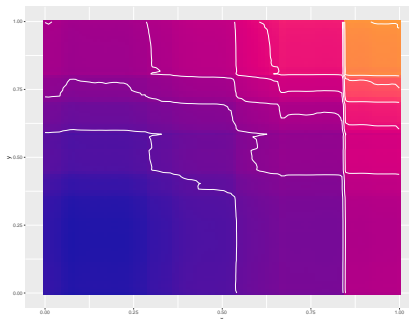
We also considered a two dimensional Poisson process with intensity  $\lambda(x, y) = 1000 e^{x^2+y^2}$  for  $x, y \in [0, 1]$ . The outcomes of the algorithm and kernel smoothing are illustrated in Figure 4 and Tables 7-8. The results demonstrate that the proposed algorithm performs well in this setting and are competitive with the kernel method. In this scenario the hyperparameter  $\beta$  has been set equal to 1. The convergence criteria indicate convergence of the simulated chains (see supplementary material).



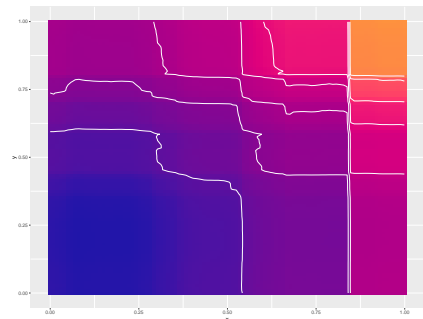
(a) Original Intensity



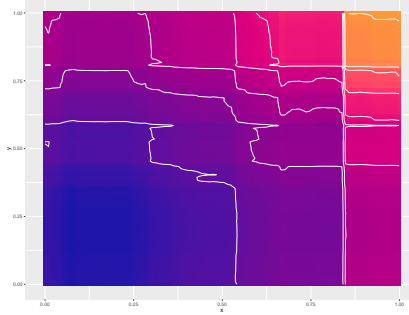
(b) Realization of Process consisting of 2176 points



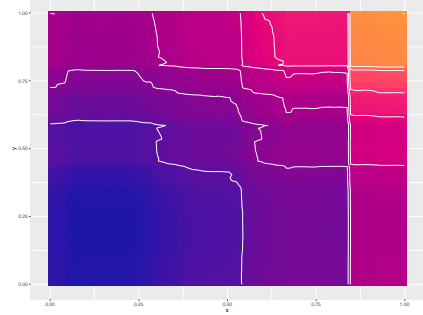
(c) Posterior Mean for 8 Trees



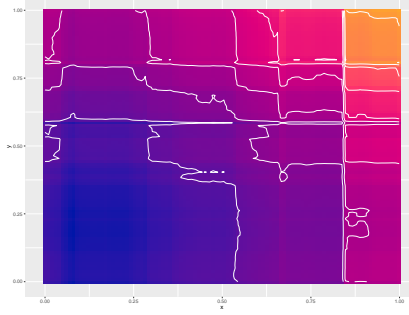
(d) Posterior Median for 8 Trees



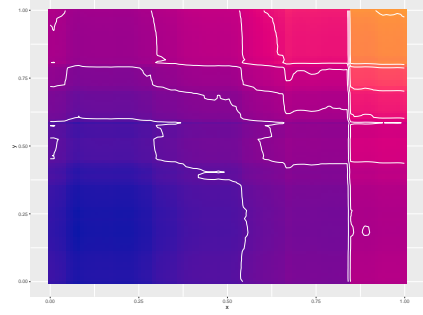
(e) Posterior Mean for 10 Trees



(f) Posterior Median for 10 Trees



(g) Posterior Mean for 15 Trees



(h) Posterior Median for 15 Trees

Figure 4: Posterior Mean and Posterior Median for 8, 10 and 15 Trees

Proposed Algorithm				
Number of trees	AAE for Posterior Mean	AAE for Posterior Median	RMSE for Posterior Mean	RMSE for Posterior Median
8	177.44	175.62	255.23	258.88
10	176.52	174.02	253.14	255.92
15	177.48	172.62	254.22	251.96

Table 7: Average Absolute Error and Root Mean Square Error for various number of trees for data in Fig. 4.

Kernel Smoothing		
Bandwidth (sigma)	AAE	RMSE
0.03	360.11	463.1
0.04	277.89	353.82
0.087	167.61	227.86
0.095	166.51	230.27

Table 8: Average Absolute Error and Root Mean Square Error for fixed bandwidth estimators for data in Fig. 4.

## 5 Intensity estimation for Real Data

In this section we apply our algorithm to real data sets when modeled as realizations of inhomogeneous Poisson processes in one and two dimensions. We compare our intensity estimates of one dimensional processes with those obtained by applying the Haar-Fisz algorithm on earthquake data. We observe that our algorithm and the Haar-Fisz algorithm lead to similar results. We also compare our intensity estimates of two dimensional processes with fixed-bandwidth and adaptive-bandwidth kernel estimators in which the bandwidth for each point is calculated using the inverse-square-root rule (Abramson, 1982). We note that the results of our algorithm using 10 Trees are similar to the kernel estimator having bandwidth chosen using likelihood cross-validation Loader (1999). As expected, the reconstructions of the intensity function are less smooth than those derived with kernel smoothing.

### 5.1 Coal Data

The first real data set under consideration is composed of the dates of 191 explosions which caused at least 10 occurrences of death from March 22, 1962 until March 15, 1981. The data set is available in the **R** package **boot** (Canty and Ripley, 2019) as **coal**. Figure 5 illustrates the Posterior Mean and the Posterior Median for 8 and 10 Trees. We observe that our algorithm captures the fluctuations of the rate of accidents in the period under consideration. The diagnostic criteria included in the Supplementary Material indicate that the considered chains have converged. See Adams *et al.* (2009), Gugushvili *et al.* (2018) and Lloyd *et al.* (2015) for alternative analyses.

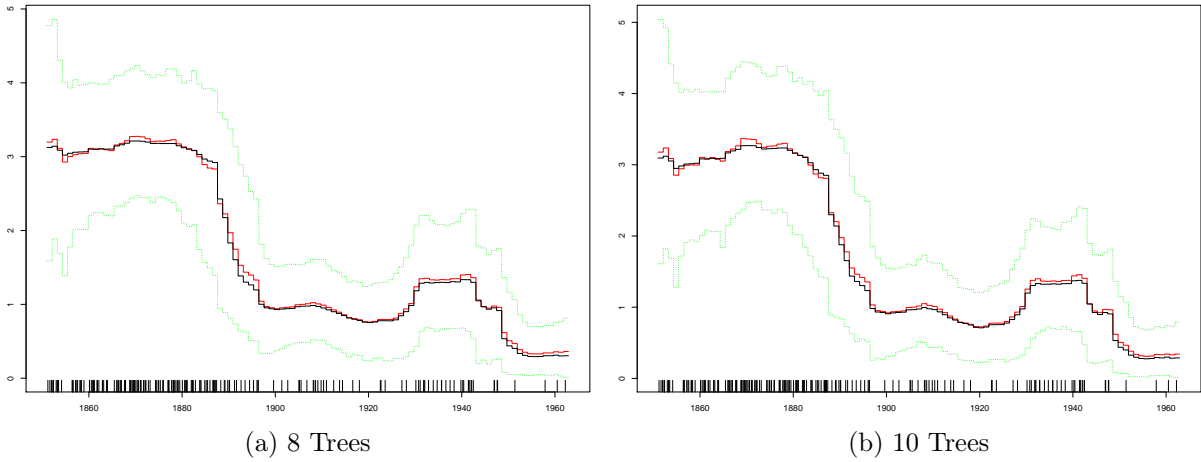


Figure 5: Coal Data: The posterior mean (red curve), the posterior median (black curve), the 95% hdi interval of the estimated intensity illustrated by the dotted green lines. The rug plot on the bottom displays the event times.

## 5.2 Earthquakes Data

This data set is available online from the Earthquake Hazards Program and consists of the times of 1088 earthquakes from 2-3-2020 to 1-4-2020. We consider the period from 27-2-2020 to 5-4-2020 to avoid edges.

Figure 6 presents the Posterior Mean and the Posterior Median for 10 Trees, as well as the intensity estimate of the Haar-Fisz algorithm applied to the counts in 128 consecutive intervals. The simulation results illustrate that our algorithm can track the varying intensity of earthquakes and is competitive with the Haar-Fisz algorithm. The diagnostic criteria included in the Supplementary Material indicate that the considered chains have converged.

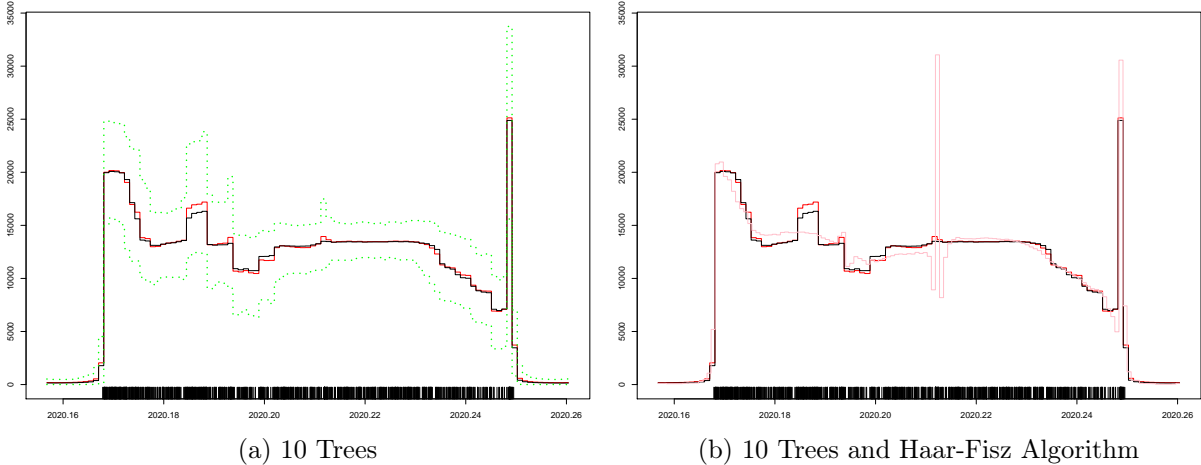


Figure 6: Earthquakes Data: The posterior mean (red curve), the posterior median (black curve), the 95% hdi interval of the estimated intensity illustrated by the dotted green lines and the intensity estimator of the Haar-Fisz Algprithm illustrated by the pink line. The rug plot on the bottom displays the event times.

### 5.3 Lansing Data

The **lansing** data set included in the **R** package **spatstat** describes the locations of different types of trees in the Lansing woods forest. Our attention is restricted to the locations of 514 maples that are presented with dots in Figures 7-8. We compare our algorithm to a fixed bandwidth estimator using a quartic kernel as suggested in Diggle *et al.* (2003). Given the tree locations, our algorithm recovers the spatial pattern of trees as rectangular regions of different intensity (Fig. 7). The results of the kernel estimators are presented in Figure 8. The diagnostic criteria included in the supplementary material indicate that the considered chains have converged for 10 Trees. However, convergence of chains is not indicated for 5 trees at some points of the testing set. We note that kernel methods are sensitive to bandwidth choice.

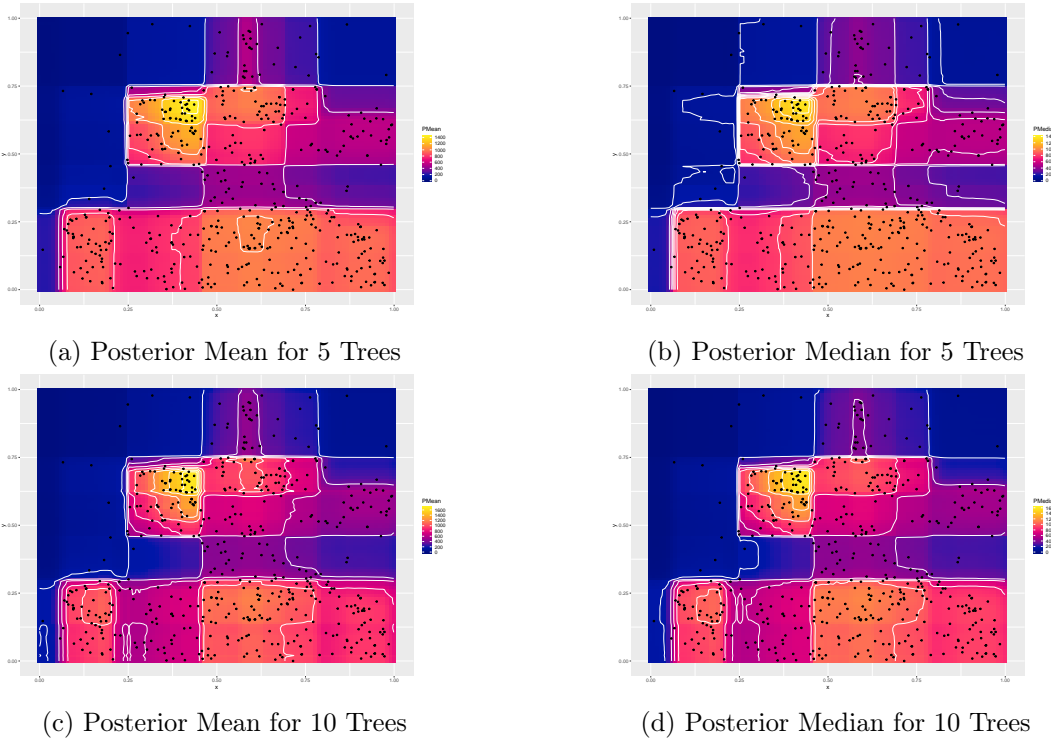


Figure 7: Posterior Mean and Posterior Median for 5 and 10 Trees

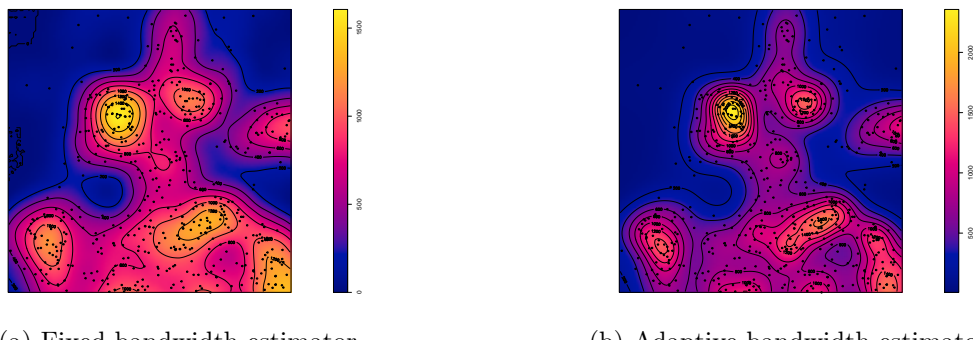


Figure 8: Fixed-bandwidth chosen using likelihood cross-validation and adaptive-bandwidth kernel estimators.

## 5.4 Redwoodfull Data

Finally, we use a data set available in the **R** package **spatstat** describing the locations of 195 trees in a square sampling region shown with dots in the figures below. Adams *et al.* (2009) analyzed the **redwoodfull** data using their recommended algorithm. We present the posterior mean and the posterior median obtained with our algorithm for different number of trees and the result of kernel estimators. Intensity inference via posterior mean (Figure 9c) or posterior median (Figure 9d) for 10 Trees is similar to the fixed-bandwidth kernel estimator with edge correction and bandwidth selected using likelihood cross-validation (Figure 10a), and the inference from Adams *et al.* (2009).

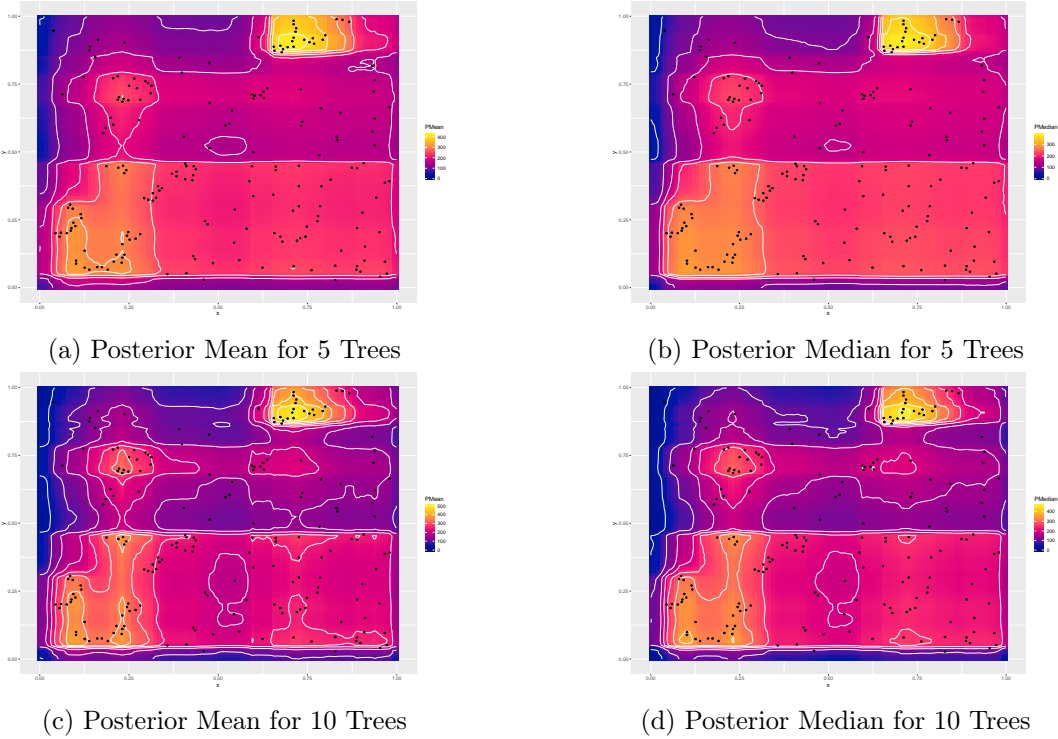


Figure 9: Posterior Mean and Posterior Median for 3, 5 and 10 Trees

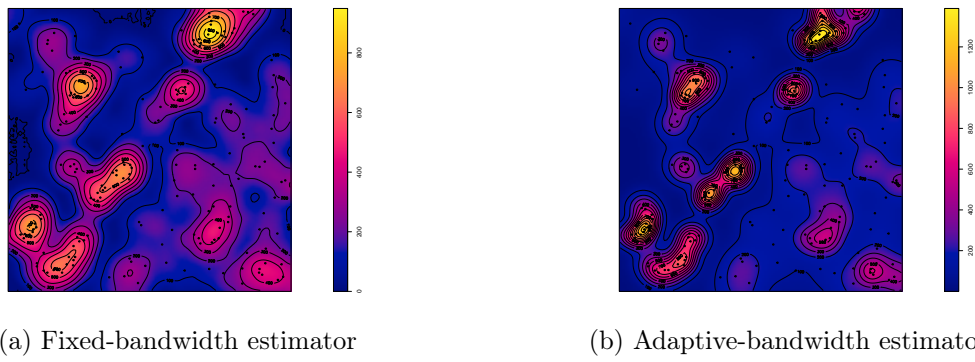


Figure 10: Fixed-bandwidth chosen using likelihood cross-validation and adaptive-bandwidth kernel estimators.

## 6 Discussion

In this article we have studied how the Bayesian Additive Regression Trees (BART) model can be applied to estimating the intensity of Poisson processes. Our approach enables full posterior inference of the intensity in a nonparametric regression setting. The simulation study on synthetic data sets shows that our algorithm can detect change points and provides good estimates of the intensity via either the posterior mean or the posterior median. Our algorithm is competitive with the Haar-Fisz algorithm and kernel methods. We also demonstrate that our inference for the intensity is consistent with the variability of the rate of events in real and synthetic data. The convergence criteria included in the supplementary material indicate good convergence of the considered chains. We ran each chain for at least 100000 iterations in order to increase our confidence in the results. However, our algorithm works well with considerably fewer iterations (around 10000).

One drawback of our algorithm is its computational cost compared to other methods. The computational cost increases with the number of trees. However, our numerical experiments show that our algorithm approximates well the intensity of Poisson processes with ensembles of less than 10 trees. The smaller number of trees decreases the computational cost. Further improvements in computational cost are beyond the scope of this article and are the topic of future work.

## References

Abramson, I. S. (1982) On bandwidth variation in kernel estimates-a square root law. *The annals of Statistics*, 1217–1223.

Adams, R. P., Murray, I. and MacKay, D. J. (2009) Tractable nonparametric bayesian inference in poisson processes with gaussian process intensities. In *Proceedings of the 26th Annual International Conference on Machine Learning*, 9–16. ACM.

Arjas, E. and Gasbarra, D. (1994) Nonparametric bayesian inference from right censored survival data, using the gibbs sampler. *Statistica sinica*, 505–524.

Baddeley, A. and Turner, R. (2005) spatstat: An R package for analyzing spatial point patterns. *Journal of Statistical Software*, **12**, 1–42. URL <http://www.jstatsoft.org/v12/i06/>.

Bleich, J. and Kapelner, A. (2014) Bayesian additive regression trees with parametric models of heteroskedasticity. *arXiv preprint arXiv:1402.5397*.

Bleich, J., Kapelner, A., George, E. I., Jensen, S. T. *et al.* (2014) Variable selection for bart: an application to gene regulation. *The Annals of Applied Statistics*, **8**, 1750–1781.

Canty, A. and Ripley, B. D. (2019) *boot: Bootstrap R (S-Plus) Functions*. R package version 1.3-22.

Chipman, H. A., George, E. I., McCulloch, R. E. and Shively, T. S. (2016) High-dimensional nonparametric monotone function estimation using bart. *arXiv preprint arXiv:1612.01619*.

Chipman, H. A., George, E. I., McCulloch, R. E. *et al.* (2010) Bart: Bayesian additive regression trees. *The Annals of Applied Statistics*, **4**, 266–298.

Daley, D. J. and Vere-Jones, D. (2003) *Elementary theory and methods*. Springer.

Davies, T. M. and Baddeley, A. (2018) Fast computation of spatially adaptive kernel estimates. *Statistics and Computing*, **28**, 937–956.

Diggle, P. J. *et al.* (2003) *Statistical analysis of spatial point patterns*. 2nd ed., Academic press.

Fryzlewicz, P. (2010) *haarfisz: Software to perform Haar Fisz transforms*. URL <https://CRAN.R-project.org/package=haarfisz>. R package version 4.5.

Fryzlewicz, P. and Nason, G. P. (2004) A haar-fisz algorithm for poisson intensity estimation. *Journal of computational and graphical statistics*, **13**, 621–638.

Gelman, A., Rubin, D. B. *et al.* (1992) Inference from iterative simulation using multiple sequences. *Statistical science*, **7**, 457–472.

Gugushvili, S., van der Meulen, F., Schauer, M. and Spreij, P. (2018) Fast and scalable non-parametric bayesian inference for poisson point processes. *arXiv preprint arXiv:1804.03616*.

Heikkinen, J. and Arjas, E. (1998) Non-parametric bayesian estimation of a spatial poisson intensity. *Scandinavian Journal of Statistics*, **25**, 435–450.

Hill, J. L. (2011) Bayesian nonparametric modeling for causal inference. *Journal of Computational and Graphical Statistics*, **20**, 217–240.

Kapelner, A. and Bleich, J. (2013) bartmachine: Machine learning with bayesian additive regression trees. *arXiv preprint arXiv:1312.2171*.

Kindo, B. P., Wang, H. and Peña, E. A. (2016) Multinomial probit bayesian additive regression trees. *Stat*, **5**, 119–131.

Lakshminarayanan, B., Roy, D. and Teh, Y. W. (2015) Particle gibbs for bayesian additive regression trees. In *Artificial Intelligence and Statistics*, 553–561.

Lewis, P. W. and Shedler, G. S. (1979) Simulation of nonhomogeneous poisson processes by thinning. *Naval research logistics quarterly*, **26**, 403–413.

Linero, A. R. (2018) Bayesian regression trees for high-dimensional prediction and variable selection. *Journal of the American Statistical Association*, **113**, 626–636.

Linero, A. R. and Yang, Y. (2018) Bayesian regression tree ensembles that adapt to smoothness and sparsity. *Journal of the Royal Statistical Society: Series B (Statistical Methodology)*, **80**, 1087–1110.

Lloyd, C., Gunter, T., Osborne, M. and Roberts, S. (2015) Variational inference for gaussian process modulated poisson processes. In *International Conference on Machine Learning*, 1814–1822.

Loader, C. (1999) Local regression and likelihood springer: New york.

Makowski, D., Ben-Shachar, M. and Lüdecke, D. (2019) bayestestr: Describing effects and their uncertainty, existence and significance within the bayesian framework. *Journal of Open Source Software*, **4**, 1541.

Murray, J. S. (2017) Log-linear bayesian additive regression trees for categorical and count responses. *arXiv preprint arXiv:1701.01503*.

Patil, P. N., Wood, A. T. *et al.* (2004) Counting process intensity estimation by orthogonal wavelet methods. *Bernoulli*, **10**, 1–24.

Pratola, M. T. *et al.* (2016) Efficient metropolis–hastings proposal mechanisms for bayesian regression tree models. *Bayesian analysis*, **11**, 885–911.

Rockova, V. and Saha, E. (2018) On theory for bart. *arXiv preprint arXiv:1810.00787*.

Rockova, V. and van der Pas, S. (2017) Posterior concentration for bayesian regression trees and their ensembles. *arXiv preprint arXiv:1708.08734*.

Scott, D. (2008) *Histograms: Theory and Practice*, 47–94.

Sparapani, R. A., Logan, B. R., McCulloch, R. E. and Laud, P. W. (2016) Nonparametric survival analysis using bayesian additive regression trees (bart). *Statistics in medicine*, **35**, 2741–2753.

Wand, M. (1997) Data-based choice of histogram bin width. *The American Statistician*, **51**, 59–64.

Zhang, J. L. and Härdle, W. K. (2010) The bayesian additive classification tree applied to credit risk modelling. *Computational Statistics & Data Analysis*, **54**, 1197–1205.

## A Appendix A: Metropolis Hastings Proposals

We describe here the proposals of Algorithm 2. The Hastings ratio can be expressed as the product of three terms (Kapelner and Bleich, 2013):

- Transition Ratio:

$$TR = \frac{q(T_j^{(t)}|T_j^*)}{q(T_j^*|T_j^{(t)})}$$

- Likelihood Ratio:

$$LR = \frac{P(s_1, \dots, s_n|T_j^*, T_{(j)}, \Lambda_{(j)})}{P(s_1, \dots, s_n|T_j^{(t)}, T_{(j)}, \Lambda_{(j)})}$$

- Tree Structure Ratio:

$$TSR = \frac{P(T_j^*)}{P(T_j^{(t)})}$$

### A.1 GROW Proposal

This proposal randomly picks a terminal node, splits the chosen terminal into two new nodes and assigns a decision rule to it.

Let  $\eta$  be the randomly picked terminal node in tree  $T_j^{(t)}$ . We denote the new nodes as  $\eta_L$  and  $\eta_R$ . We now derive the expressions for the transition ratio (TR), tree structure ratio (TSR) and likelihood ratio (LR).

**Transition Ratio** It holds that:

$$\begin{aligned} (i) \quad q(T_j^*|T_j^{(t)}) &= P(\text{GROW}) \\ &\quad \times P(\text{selecting a leaf } \eta \text{ to grow from}) \\ &\quad \times P(\text{selecting an available dimension } j \text{ to split on}) \\ &\quad \times P(\text{selecting the slitting value given the chosen dimension to split on}) \\ &= P(\text{GROW}) \frac{1}{b_j} \frac{1}{\text{card}(k_\eta)} \frac{1}{\text{card}(\tau_\eta)} \end{aligned}$$

where  $b_j$  is the number of terminal nodes in the tree  $T_j^{(t)}$ ,  $k_\eta$  the set of all available dimensions to split the node  $\eta$ ,  $\tau_\eta$  the set of all available splitting values given the chosen dimension for splitting the node  $\eta$  and  $\text{card}(S)$  the cardinality of a set  $S$ .

$$\begin{aligned} (ii) \quad q(T_j^{(t)}|T_j^*) &= P(\text{PRUNE}) \\ &\quad \times P(\text{selecting a node } \eta \text{ having two terminal nodes to prune from}) \\ &= P(\text{PRUNE}) \frac{1}{w^*} \end{aligned}$$

where  $w^*$  is the number of internal nodes with two terminal nodes as children in the tree  $T_j^*$ .

Hence the transition ratio is given by

$$TR = \frac{P(\text{PRUNE}) \frac{1}{w^*}}{P(\text{GROW}) \frac{1}{b_j} \frac{1}{\text{card}(k_\eta)} \frac{1}{\text{card}(\tau_\eta)}}.$$

**Tree Structure Ratio:** The difference between the structures of the proposed tree  $T_j^{(t)}$  and the tree  $T_j^*$  is the two offsprings  $\eta_L$  and  $\eta_R$ . Thus the tree structure ratio is:

$$\begin{aligned} TSR &= \frac{P(T_j^*)}{P(T_j^{(t)})} = \frac{(1 - p_{\text{SPLIT}}(\eta_L))(1 - p_{\text{SPLIT}}(\eta_R))p_{\text{SPLIT}}(\eta)p_{\text{RULE}}(\eta)}{(1 - p_{\text{SPLIT}}(\eta))} \\ &= \frac{\left(1 - \frac{\gamma}{(1+d(\eta_L))^\delta}\right)\left(1 - \frac{\gamma}{(1+d(\eta_R))^\delta}\right)\frac{\gamma}{(1+d(\eta))^\delta}\frac{1}{\text{card}(k_\eta)}\frac{1}{\text{card}(\tau_\eta)}}{1 - \frac{\gamma}{(1+d(\eta))^\delta}}, \end{aligned}$$

where  $p_{\text{SPLIT}}(\eta)$  is the splitting probability for a node  $\eta$  and  $p_{\text{RULE}}(\eta)$  the distribution of decision rule associated to node  $\eta$ .

**Likelihood Ratio:** The likelihood ratio is an application of the equation 8 twice, that is once considering the proposed tree,  $T_j^*$  (numerator) and the other considering the tree of the current iteration  $t$ ,  $T_j^{(t)}$  (denominator), which can be simplified as follows

$$\begin{aligned} LR &= \frac{\beta^\alpha}{\Gamma(\alpha)} \frac{\frac{\Gamma(n_{j\eta_L} + \alpha)}{(c_{j\eta_L} + \beta)^{n_{j\eta_L} + \alpha}} \frac{\Gamma(n_{j\eta_R} + \alpha)}{(c_{j\eta_R} + \beta)^{n_{j\eta_R} + \alpha}}}{\frac{\Gamma(n_{j\eta} + \alpha)}{(c_{j\eta} + \beta)^{n_{j\eta} + \alpha}}} \\ &= \frac{\beta^\alpha}{\Gamma(\alpha)} \frac{\Gamma(n_{j\eta_L} + \alpha)\Gamma(n_{j\eta_R} + \alpha)}{\Gamma(n_{j\eta} + \alpha)} \frac{(c_{j\eta} + \beta)^{n_{j\eta} + \alpha}}{(c_{j\eta_L} + \beta)^{n_{j\eta_L} + \alpha}(c_{j\eta_R} + \beta)^{n_{j\eta_R} + \alpha}} \end{aligned}$$

## A.2 PRUNE Proposal

This proposal randomly picks a parent of two terminal nodes and turns it into a terminal node by collapsing the nodes below it.

Let  $\eta$  be the picked parent of two terminal nodes,  $y$  and  $c$  the dimension and splitting value of the rule linked to the node  $\eta$ .

**Transition Ratio:** It holds that:

$$\begin{aligned} (i) \quad q(T_j^*|T_j^{(t)}) &= P(\text{PRUNE}) \\ &\quad \times P(\text{selecting a parent of two terminal nodes to prune from}) \\ &= P(\text{PRUNE}) \frac{1}{w} \end{aligned}$$

where  $w$  is the number of nodes with two terminal nodes as children in the tree  $T_j^{(t)}$ .

$$\begin{aligned} (ii) \quad q(T_j^{(t)}|T_j^*) &= P(\text{GROW}) \\ &\quad \times P(\text{selecting the node } \eta \text{ to grow from}) \\ &\quad \times P(\text{selecting the dimension } y) \\ &\quad \times P(\text{selecting the splitting value } c \text{ given the chosen dimension } y) \\ &= P(\text{GROW}) \frac{1}{w^*} \frac{1}{\text{card}(k_\eta)} \frac{1}{\text{card}(\tau_\eta)} \end{aligned}$$

where  $w^*$  is the number of terminal nodes in the tree  $T_j^*$ ,  $k_h$  the set of all available dimensions to split the node  $\eta$  and  $\tau_\eta$  the set of all available splitting values given the chosen dimension  $y$  for splitting the node  $\eta$ .

Hence the transition ratio is given by

$$TR = \frac{P(\text{GROW}) \frac{1}{w^*} \frac{1}{\text{card}(k_\eta)} \frac{1}{\text{card}(\tau_\eta)}}{P(\text{PRUNE}) \frac{1}{w}}.$$

**Tree Structure Ratio:** The proposed tree differs by not having the two children nodes  $\eta_L$  and  $\eta_R$ . Thus the tree structure ratio is:

$$\begin{aligned} TSR &= \frac{P(T_j^*)}{P(T_j^{(t)})} = \frac{(1 - p_{\text{SPLIT}}(\eta))}{(1 - p_{\text{SPLIT}}(\eta_L))(1 - p_{\text{SPLIT}}(\eta_R)) p_{\text{SPLIT}}(\eta) p_{\text{RULE}}(\eta)} \\ &= \frac{1 - \frac{\gamma}{(1+d(\eta))^{\delta}}}{\left(1 - \frac{\gamma}{(1+d(\eta_L))^{\delta}}\right) \left(1 - \frac{\gamma}{(1+d(\eta_R))^{\delta}}\right) \frac{\gamma}{(1+d(\eta))^{\delta}} \text{card}(k_{\eta}) \text{card}(\tau_{\eta})} \end{aligned}$$

**Likelihood Ratio:** Similar to the GROW proposal, the likelihood ratio can be written as follows

$$\begin{aligned} LR &= \left(\frac{\beta^{\alpha}}{\Gamma(\alpha)}\right)^{-1} \frac{\frac{\Gamma(n_{j\eta} + \alpha)}{(c_{j\eta} + \beta)^{n_{j\eta} + \alpha}}}{\frac{\Gamma(n_{j\eta_L} + \alpha)}{(c_{j\eta_L} + \beta)^{n_{j\eta_L} + \alpha}} \frac{\Gamma(n_{j\eta_R} + \alpha)}{(c_{j\eta_R} + \beta)^{n_{j\eta_R} + \alpha}}} \\ &= \left(\frac{\beta^{\alpha}}{\Gamma(\alpha)}\right)^{-1} \frac{\Gamma(n_{j\eta} + \alpha)}{\Gamma(n_{j\eta_L} + \alpha)\Gamma(n_{j\eta_R} + \alpha)} \frac{(c_{j\eta_L} + \beta)^{n_{j\eta_L} + \alpha}(c_{j\eta_R} + \beta)^{n_{j\eta_R} + \alpha}}{(c_{j\eta} + \beta)^{n_{j\eta} + \alpha}} \end{aligned}$$

### A.3 CHANGE Proposal

This proposal randomly picks an internal node and randomly reassigns to it a splitting rule.

Let  $\eta$  be the picked internal node having rule  $y < c$  and children denoted as  $\eta_R$  and  $\eta_L$ . We assume that  $\tilde{y} < \tilde{c}$  is its new assigned rule in the proposed tree,  $T_j^*$ . Following Kapelner and Bleich (2013), for simplicity we are restricted to picking an internal node having two terminal nodes as children.

**Transition Ratio:** It holds that:

- (i)  $q(T_j^* | T_j^{(t)}) = P(\text{CHANGE})$ 
  - $\times P(\text{selecting an internal node } \eta \text{ to change})$
  - $\times P(\text{selecting the new available dimension } \tilde{y} \text{ to split on})$
  - $\times P(\text{selecting the new splitting value } \tilde{c} \text{ given the chosen dimension } \tilde{y})$
- (ii)  $q(T_j^{(t)} | T_j^*) = P(\text{CHANGE})$ 
  - $\times P(\text{selecting the node } \eta \text{ to change})$
  - $\times P(\text{selecting the dimension } y \text{ to split on})$
  - $\times P(\text{selecting the splitting value } c \text{ given the chosen dimension } y)$

Thus the Transition Ratio is

$$TR = \frac{P(\text{selecting } c \text{ to split on given the chosen dimension } y)}{P(\text{selecting } \tilde{c} \text{ to split on given the chosen dimension } \tilde{y})}$$

**Tree Structure Ratio:** The two trees differ in the splitting rule at node  $\eta$ . Thus we have that

$$\begin{aligned} TSR &= \frac{P(T_j^*)}{P(T_j^{(t)})} = \frac{p_{\text{SPLIT}}(\eta) p_{\text{RULE}}(\eta|T_j^*)}{p_{\text{SPLIT}}(\eta) p_{\text{RULE}}(\eta|T_j^{(t)})} \\ &= \frac{P(\text{selecting } \tilde{y}) P(\text{selecting } \tilde{c} \text{ given } \tilde{y})}{P(\text{selecting } y) P(\text{selecting } c \text{ given } y)} \\ &= \frac{P(\text{selecting } \tilde{c} \text{ given } \tilde{y})}{P(\text{selecting } c \text{ given } y)}. \end{aligned}$$

It then follows that  $TR \cdot TSR = 1$ , and hence only the likelihood ratio needs to be found to obtain the Hastings ratio.

**Likelihood Ratio:** Let  $n_L^* = n_{j\eta_L}^{(T_j^*)}$ ,  $n_R^* = n_{j\eta_R}^{(T_j^*)}$ ,  $c_L^* = c_{j\eta_L}^{(T_j^*)}$ ,  $c_R^* = c_{j\eta_R}^{(T_j^*)}$ ,  $n_L^{(t)} = n_{j\eta_L}^{(T_j^{(t)})}$ ,  $n_R^{(t)} = n_{j\eta_R}^{(T_j^{(t)})}$ ,  $c_L^{(t)} = c_{j\eta_L}^{(T_j^{(t)})}$  and  $c_R^{(t)} = c_{j\eta_R}^{(T_j^{(t)})}$ , where  $(T_j^*)$  and  $(T_j^{(t)})$  indicate that the corresponding quantities are related to the tree  $T_j^*$  and  $T_j^{(t)}$  respectively. Following the previous proposals, the likelihood ratio is

$$LR = \frac{\frac{\Gamma(n_L^* + \alpha)}{(c_L^* + \beta)^{n_L^* + \alpha}} \frac{\Gamma(n_R^* + \alpha)}{(c_R^* + \beta)^{n_R^* + \alpha}}}{\frac{\Gamma(n_L^{(t)} + \alpha)}{(c_L^{(t)} + \beta)^{n_L^{(t)} + \alpha}} \frac{\Gamma(n_R^{(t)} + \alpha)}{(c_R^{(t)} + \beta)^{n_R^{(t)} + \alpha}}} = \frac{(c_L^{(t)} + \beta)^{n_L^{(t)} + \alpha} (c_R^{(t)} + \beta)^{n_R^{(t)} + \alpha}}{(c_L^* + \beta)^{n_L^* + \alpha} (c_R^* + \beta)^{n_R^* + \alpha}} \frac{\Gamma(n_L^* + \alpha) \Gamma(n_R^* + \alpha)}{\Gamma(n_L^{(t)} + \alpha) \Gamma(n_R^{(t)} + \alpha)}.$$

## B Appendix B: The Poisson Process conditional likelihood

Let us consider a finite realization of an inhomogeneous Poisson process with  $n$  points  $s_1, \dots, s_n$ . Given the tree components  $(T, \Lambda)$ , and approximating the intensity of a point  $s_i \in S$  by a product of  $m$  trees  $\lambda(s_i) = \prod_{j=1}^m g(s_i; T_j, \Lambda_j)$ , the likelihood is:

$$\begin{aligned} P(s_1, \dots, s_n | \Lambda, T) &= \prod_{i=1}^n \lambda(s_i) \exp \left( - \int_S \lambda(s) ds \right) \\ &= \prod_{i=1}^n \prod_{j=1}^m g(s_i; T_j, \Lambda_j) \exp \left( - \int_S \prod_{j=1}^m g(s; T_j, \Lambda_j) ds \right). \end{aligned} \quad (12)$$

The first term of the above equation can be written as follows

$$\begin{aligned} \prod_{i=1}^n \prod_{j=1}^m g(s_i; T_j, \Lambda_j) &= \prod_{i=1}^n \prod_{j=1, j \neq h}^m g(s_i; T_j, \Lambda_j) g(s_i; T_h, \Lambda_h) \\ &= \prod_{i=1}^n \prod_{j=1, j \neq h}^m g(s_i; T_j, \Lambda_j) \left( \prod_{i=1}^n g(s_i; T_h, \Lambda_h) \right) = c_h \prod_{t=1}^{b_h} \lambda_{ht}^{n_{ht}} \end{aligned}$$

where  $c_h = \prod_{i=1}^n \prod_{j=1, j \neq h}^m g(s_i; T_j, \Lambda_j)$  and  $n_{ht}$  is the cardinality of the set  $\{i : s_i \in \Omega_{ht}\}$ .

The exponential term of (12) can be expressed as:

$$\begin{aligned} \exp \left( - \int_S \prod_{j=1}^m g(s; T_j, \Lambda_j) ds \right) &= \exp \left( - \int_S \prod_{j=1, j \neq h}^m g(s; T_j, \Lambda_j) g(s; T_h, \Lambda_h) \right) \\ &= \exp \left( - \int_S \prod_{j=1, j \neq h}^m g(s; T_j, \Lambda_j) \left( \sum_{t=1}^{b_h} \lambda_{ht} I(s \in \Omega_{ht}) \right) ds \right) \\ &= \exp \left( - \int_S \sum_{t=1}^{b_h} \lambda_{ht} \prod_{j=1, j \neq h}^m g(s; T_j, \Lambda_j) I(s \in \Omega_{ht}) ds \right) \end{aligned}$$

Tonelli's theorem allows the change of order between summation and integral.

$$\begin{aligned} \exp \left( - \int_S \prod_{j=1}^m g(s; T_j, \Lambda_j) ds \right) &= \exp \left( - \sum_{t=1}^{b_h} \lambda_{ht} \int_S \prod_{j=1, j \neq h}^m g(s; T_j, \Lambda_j) I(s \in \Omega_{ht}) ds \right) \\ &= \exp \left( - \sum_{t=1}^{b_h} \lambda_{ht} c_{ht} \right) \end{aligned}$$

where

$$c_{ht} = \int_S \left( \prod_{j=1, j \neq h}^m g(s; T_j, \Lambda_j) \right) I(s \in \Omega_{ht}) ds.$$

Let  $T_{(h)} = \{T_j\}_{j=1, j \neq h}^m$  be an ensemble of trees not including the tree  $T_h$  that defines the global partition  $\{\bar{\Omega}_k^{(h)}\}_{k=1}^{K(T_{(h)})}$  by merging all cuts in  $\{T_j\}_{j=1, j \neq h}^m$ . Giving,

$$\prod_{j=1, j \neq h}^m g(s; T_j, \Lambda_j) = \sum_{k=1}^{K(T_{(h)})} \bar{\lambda}_k^{(h)} I(s \in \bar{\Omega}_k^{(h)})$$

where

$$\bar{\lambda}_k^{(h)} = \prod_{t=1, t \neq h}^m \prod_{l=1}^{b_t} \lambda_{tl}^{I(\Omega_{tl} \cap \bar{\Omega}_k^{(h)} \neq 0)},$$

leading to the following expression for  $c_{ht}$ ,

$$\begin{aligned} c_{ht} &= \int_S \left( \prod_{j=1, j \neq h}^m g(s, T_j, \Lambda_j) \right) I(s \in \Omega_{ht}) ds = \int_S \left( \sum_{k=1}^{K(T_{(h)})} \bar{\lambda}_k^{(h)} I(s \in \bar{\Omega}_k^{(h)}) \right) I(s \in \Omega_{ht}) ds \\ &= \sum_{k=1}^{K(T_{(h)})} \bar{\lambda}_k^{(h)} \int_S I(s \in \bar{\Omega}_k^{(h)} \cap \Omega_{ht}) ds = \sum_{k=1}^{K(T_{(h)})} \bar{\lambda}_k^{(h)} |\bar{\Omega}_k^{(h)} \cap \Omega_{ht}|, \end{aligned}$$

where  $|\bar{\Omega}_k^{(h)} \cap \Omega_{ht}|$  is the volume of the region  $\bar{\Omega}_k^{(h)} \cap \Omega_{ht}$ . Hence the conditional likelihood can be written as follows

$$P(s_1, \dots, s_n | \Lambda, T) = c_h \prod_{t=1}^{b_h} \lambda_{ht}^{n_{ht}} e^{-\lambda_{ht} c_{ht}}.$$

## C Appendix C: The conditional integrated likelihood

The conditional integrated likelihood is given by

$$\begin{aligned}
P(s_1, \dots, s_n | T_h, T_{(h)}, \Lambda_{(h)}) &= \int P(s_1, \dots, s_n, \Lambda_h | T_h, T_{(h)}, \Lambda_{(h)}) d\Lambda_h \\
&= \int P(s_1, \dots, s_n | \Lambda, T) P(\Lambda_h | T_h, T_{(h)}, \Lambda_{(h)}) d\Lambda_h \\
&= c_h \int \dots \int \prod_{t=1}^{b_h} \lambda_{ht}^{n_{ht}} e^{-\lambda_{ht} c_{ht}} \prod_{t=1}^{b_h} \frac{\beta^\alpha}{\Gamma(\alpha)} e^{-\beta \lambda_{ht}} \lambda_{ht}^{\alpha-1} d\lambda_{h1} \dots d\lambda_{hb_h} \\
&= c_h \left( \frac{\beta^\alpha}{\Gamma(\alpha)} \right)^{b_h} \prod_{t=1}^{b_h} \int \lambda_{ht}^{n_{ht} + \alpha - 1} e^{-(c_{ht} + \beta) \lambda_{ht}} d\lambda_{ht} \\
&= c_h \left( \frac{\beta^\alpha}{\Gamma(\alpha)} \right)^{b_h} \prod_{t=1}^{b_h} \frac{\Gamma(n_{ht} + \alpha)}{(c_{ht} + \beta)^{n_{ht} + \alpha}}
\end{aligned}$$

## D Appendix D: The model for the case of one tree

The proposed model for considering only one tree can be written as follows

$$\lambda(s_i) = g(s_i; T, \Lambda) = \sum_{k=1}^b \lambda_k I(s_i \in \Omega_k)$$

$$\begin{aligned} T &\sim \text{heterogeneous Galton-Watson process for a partition of } S \\ \lambda_k | T &\sim \text{Gamma}(\alpha, \beta) \end{aligned}$$

underpinned by a tree-shaped partition  $T = \{\Omega_k\}_{k=1}^b$  where  $b$  is the number of terminal nodes in the tree  $T$ . Each leaf node  $k$  associated to region  $\Omega_k$  is linked with a parameter  $\lambda_k$ . All parameters  $\lambda_k$  are collected in the vector  $\Lambda = (\lambda_1, \lambda_2, \dots, \lambda_b)$ . The parameters of the model are

1. the regression tree  $T$
2. the parameters  $\Lambda = (\lambda_1, \lambda_2, \dots, \lambda_b)$ .

We assume that the leaf parameters are independent, i.e.,  $P(\Lambda|T) = \prod_{k=1}^b P(\lambda_k|T)$ .

### D.1 Poisson Process conditional likelihood

The conditional likelihood of a finite realization of an inhomogeneous Poisson process with  $n$  points  $s_1, \dots, s_n$  is derived by describing  $\lambda(s)$  using one tree  $(\Lambda, T)$  as:  $\lambda(s) = g(s; T, \Lambda)$ .

$$P(s_1, \dots, s_n | \Lambda, T) = \prod_{i=1}^n \lambda(s_i) \exp \left( - \int_S \lambda(s) ds \right) = \prod_{i=1}^n g(s_i; T, \Lambda) \exp \left( - \int_S g(s; T, \Lambda) ds \right). \quad (13)$$

The first term of the above equation can be written as follows

$$\prod_{i=1}^n g(s_i; T, \Lambda) = \prod_{k=1}^b \lambda_k^{n_k}$$

where  $n_k$  is the cardinality of the set  $\{i : s_i \in \Omega_k\}$ .

The exponential term of (13) can be expressed as follows

$$\begin{aligned} \exp \left( - \int_S g(s; T, \Lambda) ds \right) &= \exp \left( - \int_S \sum_{k=1}^b \lambda_k I(s \in \Omega_k) ds \right) \\ &= \exp \left( - \sum_{k=1}^b \lambda_k \int_S I(s \in \Omega_k) ds \right) = \exp \left( - \sum_{k=1}^b \lambda_k |\Omega_k| \right) \end{aligned}$$

Hence the conditional likelihood can be written as

$$P(s_1, \dots, s_n | \Lambda, T) = \prod_{k=1}^b \lambda_k^{n_k} e^{-\lambda_k |\Omega_k|}, \quad (14)$$

where  $|\Omega_k|$  is the volume of the region  $\Omega_k$ .

## D.2 Inference Algorithm

Inference on the model parameters  $(\Lambda, T)$  induces sampling from the posterior  $P(\Lambda, T|s_1, \dots, s_n)$ . A Metropolis Hastings within Gibbs sampler (Algorithm 3) is proposed for sampling from the posterior  $P(\Lambda, T|s_1, \dots, s_n)$ . Noting that,

$$P(\Lambda, T|s_1, \dots, s_n) = P(\Lambda|T, s_1, \dots, s_n) P(T|s_1, \dots, s_n)$$

and

$$P(\Lambda|T, s_1, \dots, s_n) \propto P(s_1, \dots, s_n|\Lambda, T) P(\Lambda|T) \propto \prod_{k=1}^b \lambda_k^{n_k+\alpha-1} e^{-(|\Omega_k|+\beta)\lambda_k},$$

a draw from  $(T, \Lambda)|s_1, \dots, s_n$  can be achieved in  $(b+1)$  successive steps:

- sample  $T|n, s_1, \dots, s_n$  through Metropolis-Hastings Algorithm summarized in Algorithm 4
- sample  $\lambda_k|T, n, s_1, \dots, s_n$  from a Gamma distribution with shape equal to  $n_k+\alpha$  and rate equal to  $|\Omega_k|+\beta$  for  $k = 1, \dots, b$ .

Noting that

$$P(T|s_1, \dots, s_n) \propto P(s_1, \dots, s_n|T) P(T)$$

the integrated likelihood (integrating out the parameters  $\Lambda$ ) is:

$$\begin{aligned} P(s_1, \dots, s_n|T) &= \int P(s_1, \dots, s_n, \Lambda|T) d\Lambda = \int P(s_1, \dots, s_n|\Lambda, T) P(\Lambda|T) d\Lambda \\ &= \left( \frac{\beta^\alpha}{\Gamma(a)} \right)^b \prod_{k=1}^b \int \lambda_k^{n_k+\alpha-1} e^{-(|\Omega_k|+\beta)\lambda_k} d\lambda_k \\ &= \left( \frac{\beta^\alpha}{\Gamma(a)} \right)^b \prod_{k=1}^b \frac{\Gamma(n_k+\alpha)}{(\beta+|\Omega_k|)^{n_k+\alpha}}. \end{aligned} \quad (15)$$

In the tree sampling Algorithm 4, the transition kernel  $q$  is chosen from the three proposals: GROW, PRUNE, CHANGE (Chipman *et al.*, 2010; Kapelner and Bleich, 2013), and Eq. (15) allows us to compute the Metropolis Hastings ratio to accept or reject the proposal.

---

**Algorithm 3** Proposed Algorithm: Metropolis Hastings within Gibbs sampler

---

```

for  $t = 1, 2, 3, \dots$  do
  Sample  $T^{(t+1)}|s_1, \dots, s_n$ 
  for  $k = 1$  to  $b$  do
    Sample  $\lambda_k^{(t+1)}|s_1, \dots, s_n, T^{(t+1)}$ 
  end for
end for

```

---

---

**Algorithm 4** Metropolis Hastings Algorithm for sampling from the posterior  $P(T|s_1, \dots, s_n)$

---

Generate a candidate value  $T^*$  with probability  $q(T^*|T^{(t)})$ .

Set  $T^{(t+1)} = T^*$  with probability

$$\alpha(T^{(t)}, T^*) = \min \left( 1, \frac{q(T^{(t)}|T^*)}{q(T^*|T^{(t)})} \frac{P(s_1, \dots, s_n|T^*)}{P(s_1, \dots, s_n|T^{(t)})} \frac{P(T^*)}{P(T^{(t)})} \right)$$

Otherwise, set  $T^{(t+1)} = T^{(t)}$ .

---

## E Appendix E: Simulation results on synthetic data with various number of sampling iterations

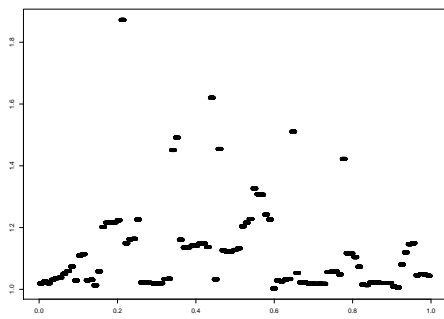
In this appendix we show that our algorithm works equally well for 10000 iterations by running three parallel chains, examining their convergence and assessing the performance of our algorithm via AAE and RMSE of computed estimates over various number of iterations. We also check the convergence of chains using the Gelman-Rubin criterion in all cases.

### E.1 One dimensional Poisson Process with stepwise intensity

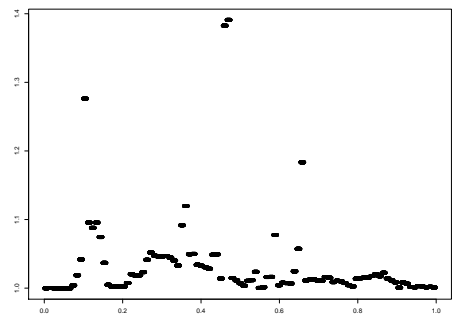
Table 9 shows that there are no significant difference in errors increasing the number of iterations from 10000 to 200000. Figure 11 reveals that the chains work less well at points close to jumps for small number of iterations.

Proposed Algorithm					
Number of trees	Number of Iterations	AAE for Posterior Mean	AAE for Posterior Median	RMSE for Posterior Mean	RMSE for Posterior Median
5	10000	284.61	274.3	588.88	590.5
	50000	289.11	284.56	575.11	579.17
	200000	279.88	269.81	572.94	576.94
7	10000	265.22	257.49	572.33	576.58
	50000	276.19	267.75	580.35	584.47
	200000	278.37	269.78	582.82	584.1

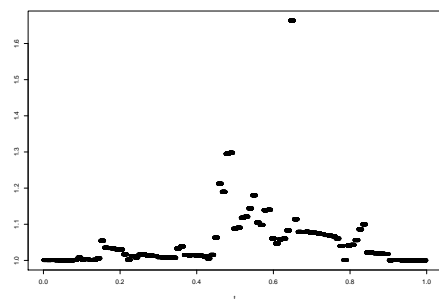
Table 9: Average Absolute Error and Root Mean Square Error for various number of iterations and trees.



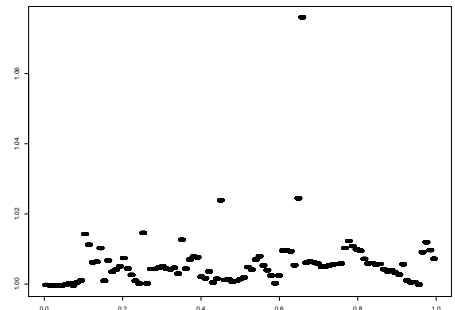
(a) 5 Trees and 10000 iterations



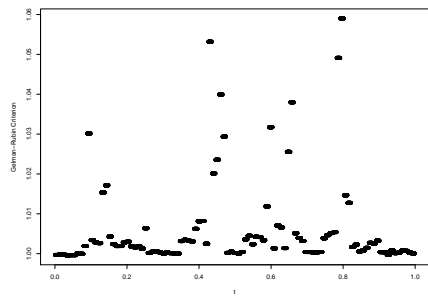
(b) 7 Trees and 10000 iterations



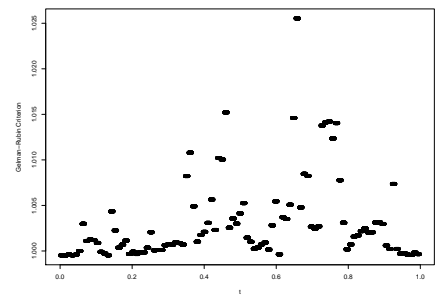
(c) 5 Trees and 50000 iterations



(d) 7 Trees and 50000 iterations



(e) 5 Trees and 200000 iterations



(f) 7 Trees and 200000 iterations

Figure 11: The Gelman-Rubin Criterion for various number of iterations and trees.

## E.2 One dimensional Poisson Process with continuously varying intensity

Table 10 shows that increasing the number of iterations does not change essentially the error for the synthetic data presented in Section 4.2. The convergence criterion indicates that even for small number of iterations, the chains converge for 10 trees. For 5 trees they converge for the majority of the range (Figure 12).

Proposed Algorithm					
Number of trees	Number of Iterations	AAE for Posterior Mean	AAE for Posterior Median	RMSE for Posterior Mean	RMSE for Posterior Median
5	10000	6.27	6.71	9.83	10.62
	50000	6.16	6.51	9.63	10.42
	100000	6.14	6.38	9.52	10.17
7	10000	5.99	6.03	9.54	9.95
	50000	6.04	6.1	9.49	9.88
	100000	5.95	6.01	9.39	9.8

Table 10: Average Absolute Error and Root Mean Square Error for various number of iterations and trees.

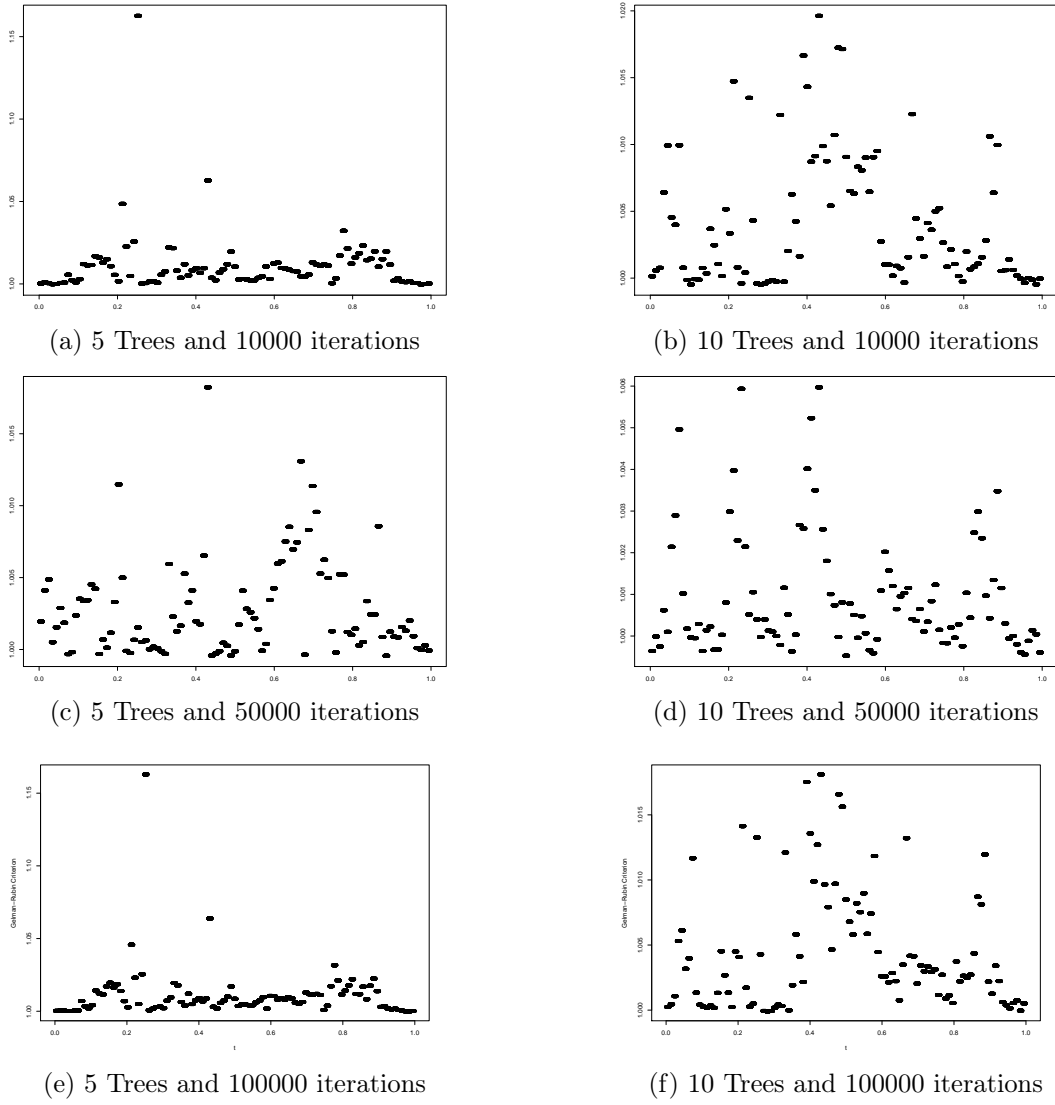


Figure 12: The Gelman-Rubin Criterion for various number of iterations and trees.

### E.3 Two dimensional Poisson process with stepwise intensity function

Likewise, we do not observe significant improvement in AAE and RMSE beyond 10000 iterations (see Table 11). Moreover, increasing the number of iterations does not fix the convergence issues at points close to jumps (see Figure 13).

Proposed Algorithm					
Number of trees	Number of Iterations	AAE for Posterior Mean	AAE for Posterior Median	RMSE for Posterior Mean	RMSE for Posterior Median
4	10000	241.82	240.1	464.99	489.93
	50000	209.95	209.58	392.43	418.37
	100000	208.74	213.04	410.19	447.86

Table 11: Average Absolute Error and Root Mean Square Error for 4 Trees and various number of iterations.

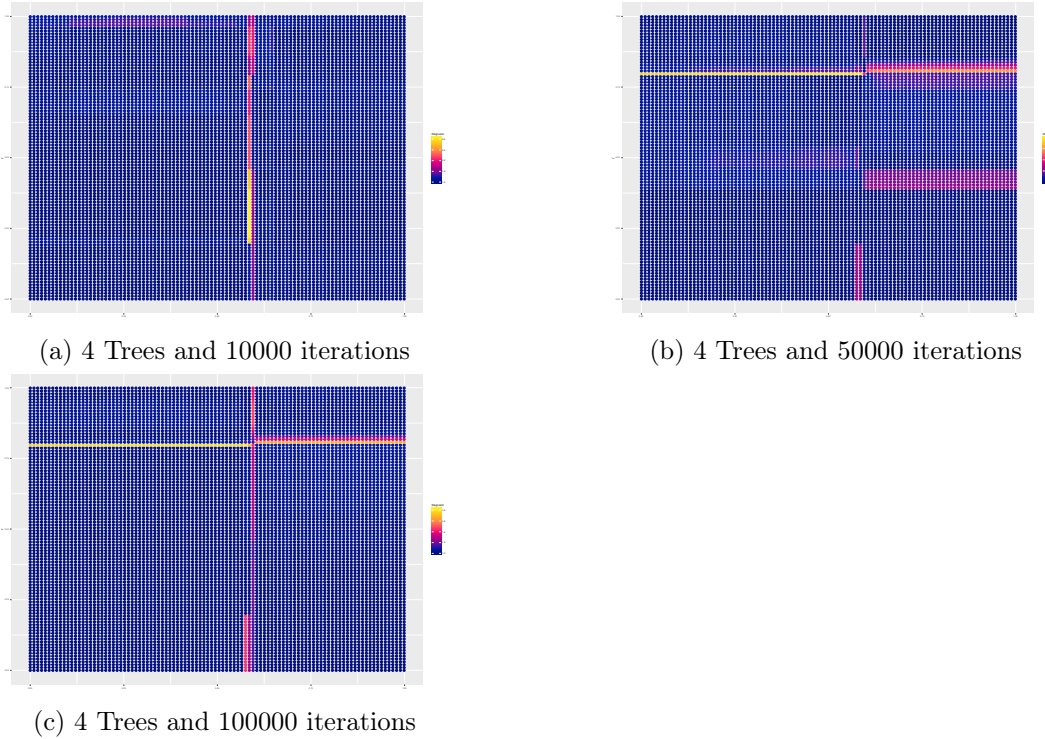


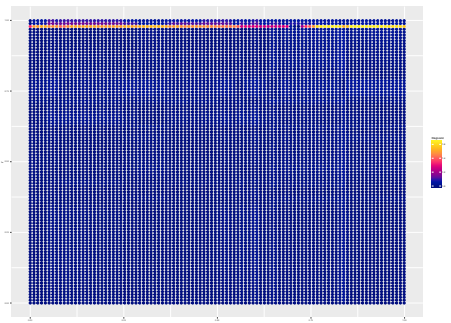
Figure 13: The Gelman-Rubin Criterion for 4 trees and various number of iterations.

#### E.4 Inhomogeneous two dimensional Poisson Process with Gaussian intensity

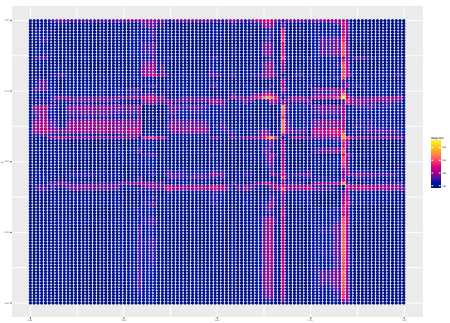
Similarly to all the above scenarios, the error with 10000 iterations are already comparable to those obtained with a larger number of iterations (see Table 12). Figure 14 shows that the chains converge for 10 Trees even if we consider a relatively small number of iterations. The same holds for the majority of testing points for 8 Trees. The algorithm only provides less accurate estimations for the testing points close to the upper end of the domain for 8 Trees and relatively small number of iterations.

Proposed Algorithm					
Number of trees	Number of Iterations	AAE for Posterior Mean	AAE for Posterior Median	RMSE for Posterior Mean	RMSE for Posterior Median
8	10000	173.02	175.61	247.5	255.81
	50000	169.54	170.5	242.03	250.74
	200000	177.44	175.62	255.23	258.88
10	10000	168.91	168.78	242.62	249.38
	50000	177.72	173.93	254.67	256.32
	200000	176.52	174.02	253.14	255.92

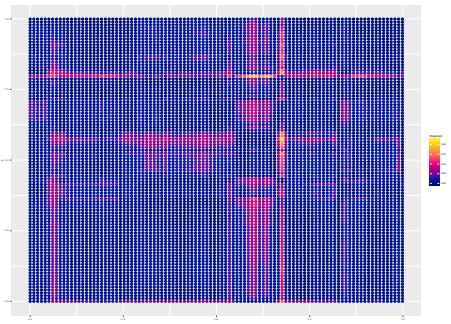
Table 12: Average Absolute Error and Root Mean Square Error for various number of iterations and trees.



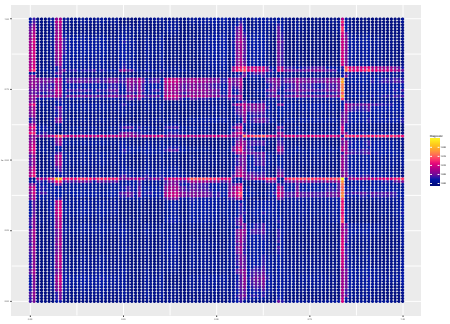
(a) 8 Trees and 10000 iterations



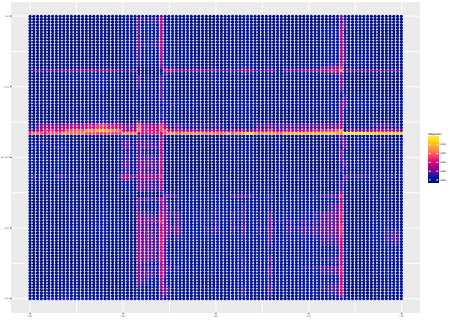
(b) 10 Trees and 10000 iterations



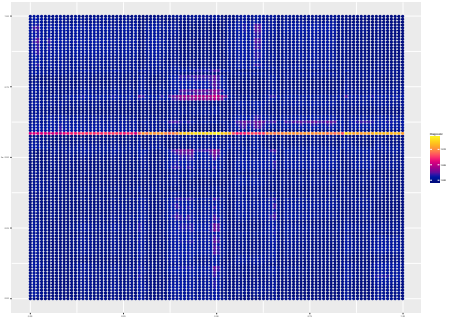
(c) 8 Trees and 50000 iterations



(d) 10 Trees and 50000 iterations



(e) 8 Trees and 200000 iterations



(f) 10 Trees and 200000 iterations

Figure 14: The Gelman-Rubin Criterion for various number of iterations and trees.